Available online at www.sciencedirect.com
SCIENCE DIRECT
ELSEVIER
Coordination Chemistry Reviews 250 (2006) 2000–2022
COORDINATION CHEMISTRY REVIEWS
www.elsevier.com/locate/ccr

Review

Homoleptic, mononuclear transition metal complexes of 1,2-dioxolenes: Updating their electrochemical-to-structural (X-ray) properties

Piero Zanello *, Maddalena Corsini

Dipartimento di Chimica dell'Università di Siena, Via Aldo Moro, 53100 Siena, Italy

Received 15 April 2005; received in revised form 5 October 2005; accepted 7 December 2005
Available online 24 January 2006

Contents

* Corresponding author. Tel.: +39 0577 234262; fax: +39 0577 234233.
E-mail address: zanello@unisi.it (P. Zanello).

0010-8545/$ – see front matter
doi:10.1016/j.ccr.2005.12.017

Abstract

This review updates the electrochemical and structural aspects of homoleptic quinoidal (or pseudo-quinoidal) molecules coordinated to (single) transition metal ions. In fact, since 1,2-dioxolenes are redox-active molecules able to shuttle reversibly through the sequence quinone/hydroquinone/catechol, their metal complexes can display both the ligand-centred and the metal-centred electron transfers, which in some cases can overlap or trigger internal charge reorganizations. Such extended electron transfer ability makes it difficult in some cases to ascertain the oxidation states of both the ligands and the metal. Joint structural and electrochemical investigation can in most cases succeed in solving the dilemma, but in a wider horizon further experimental (for instance, magnetic measurements) or theoretical supports (enlightenment on the composition of frontier orbitals) would be desirable.

Keywords: Metal complex; Electron transfer; X-ray properties

1. Introduction

The electrochemistry of quinoidal metalla-complexes has been from time to time quickly mentioned in the wider context of a continual updating of the chemical and physico-chemical properties of benzene-1,2-diolate derivatives, also inclusive of their biological relevancy [1]. We wish to focus here more in detail on the redox activity of homoleptic metalla-dioxolenes in connection with the solid-state structural changes triggered by their electron-transfer aptitude, and, when possible, also in comparison with the related aspects of the dithiolene analogs [2].

In fact, both 1,2-dioxolenes and 1,2-dithiolenes are redox active (or redox non-innocent [3]) ligands able to undergo reversibly the one-electron sequences illustrated in Scheme 1 [4].

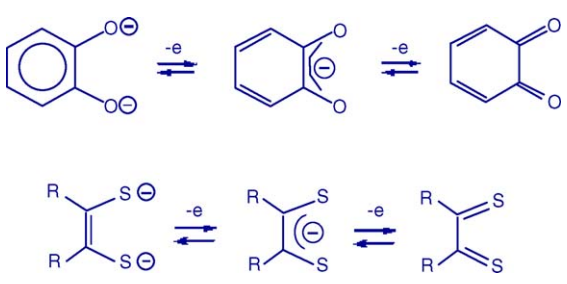

Scheme 1. The similarity between the redox aptitude of 1,2-dioxolenes and that of 1,2-dithiolenes.

Such activity can add to the redox processes of the central metal ion itself in the corresponding metal complexes, thus making it often complicated to recognize the induced charge distribution, or their ligand- or metal-centred nature. In this context, it is useful to recall that, but for a few exceptions [5], it is generally agreed that, in order to decide about the oxidation state of the quinoidal ligands of metal complexes, two bonding lengths are particularly diagnostic [1]:

- the C–O distance:
  - quinone form: C–O ≈ 1.23 Å,
  - semiquinone form: C–O ≈ 1.29 Å,
  - catecholate form: C–O ≈ 1.35 Å;
- the intradiol C1–C2 distance:
  - quinone form: C1–C2 ≈ 1.53 Å,
  - semiquinone form: C1–C2 ≈ 1.44 Å,
  - catecholate form: C1–C2 ≈ 1.39 Å;

Such bond distances are obviously in agreement with the crystallographic data of the pertinent free ligands (for instance: 1,2-dihydroxybenzene, 1,2-benzoquinone, 3,5-di-*tert*-butyl-1,2-benzoquinone, and tetrachloro-1,2-benzoquinone) [6].

A further support can arise from a statistical approach, which, taking in consideration both the C–O and all the six intraring C/C distances, affords a diagnostic structural function Δ. In the case of a pure quinonate oxidation state: $\Delta = 0$; in the case of a pure

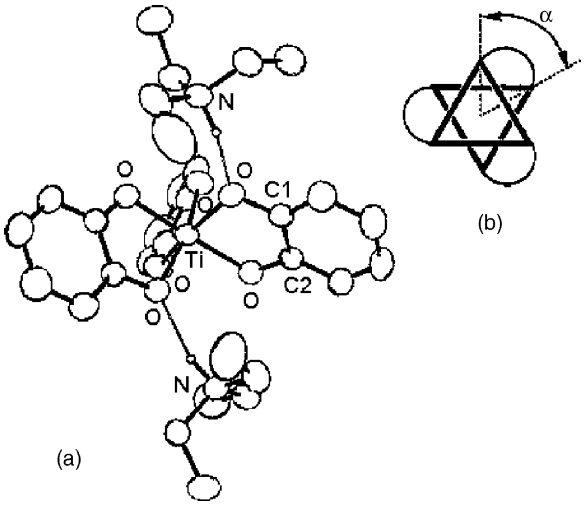

Fig. 1. X-ray crystal structure of $[Ti(1,2\text{-}O_2C_6H_4)_3]^{2-}$. $[Et_3NH]^+$ counterion. Average bond lengths: Ti–O = 1.97 Å; C–O = 1.35 Å; C1–C2 = 1.41 Å (adapted from Ref. [8]).

semiquinonate oxidation state: $\Delta = -1.0$; in the case of a pure catecholate oxidation state: $\Delta = -2.0$ [7].

Finally, we will mention non-benzenoid quinoidal-type ligands, such as squarates, croconates and tropolonates, the electrochemical-to-structural aspects of which have not yet found adequate space in literature (or, as research subjects).

2. Benzenoid ligands

2.1. Group 4 metalla-complexes (Ti, Hf)

2.1.1. Titanium complexes

2.1.1.1. Tris(quinoidal) complexes. Fig. 1 shows the molecular structure of the dianion $[Ti(1,2\text{-}O_2C_6H_4)_3]^{2-}$ [8].

Since the trigonal twist angle α (Fig. 1b) is 43.5°, the geometry is defined as pseudooctahedral (in fact, for a perfect trigonal prism (D_{3h}) α is 0°, whereas for a perfect octahedron (O_h) α is 60°).

Based on the criteria mentioned above, the catecholate nature of the dioxolene ligand is quite evident in the present complex. As a matter of fact, the C–O and C1–C2 distances are substantially coincident with those of free catechol (1,2-dihydroxybenzene) [6a], and rather different from those of free benzoquinone [6b].

In aqueous solution ($6 < pH < 12$), the red $[Ti^{IV}(Cat)_3]^{2-}$ undergoes a chemically and electrochemically reversible [4] one-electron reduction to the corresponding pale green $[Ti^{III}(Cat)_3]^{3-}$ ($E^{0\prime} = -1.38$ V versus SCE) [8]. Unfortunately, no attempts have been carried out to look at the eventual oxidation of the catechol ligands.

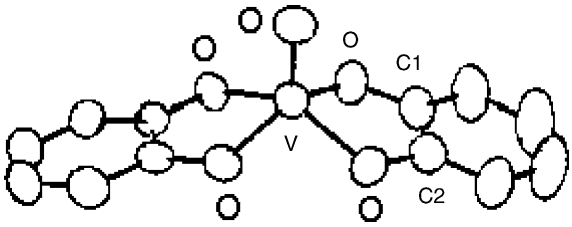

Fig. 2. X-ray crystal structure of $[VO(1,2\text{-}O_2C_6H_4)_2]^{2-}$ (adapted from Ref. [11]).

The crystal structure of the macrobicyclic tris(catecholate) dianion $[Ti^{IV}(bicapped\text{-}TRENCAM)]^{2-}$ is known [9], but since no pertinent electrochemical investigation has been carried out we will discuss the class of cyclophane ligands in Sections 2.2.1.2, 2.3.2.1, 2.5.1.1.

2.1.2. Hafnium complexes

2.1.2.1. Tetrakis(quinoidal) complexes. The tetraanion $[Hf(1,2\text{-}O_2C_6H_4)_4]^{4-}$ shows an eight-coordinate dodecahedral geometry, which will be illustrated in Section 2.10.1.1 [10]. The C–O and C1–C2 bond lengths are diagnostic for the catecholate form of the four ligands, which means that the complex can be described as $[Hf^{IV}(Cat)_4]^{4-}$. No electrochemical data are available.

2.2. Group 5 metalla-complexes (V)

2.2.1. Vanadium complexes

2.2.1.1. Bis(quinoidal) complexes. Fig. 2 shows the square pyramidal geometry of the dianion $[VO(1,2\text{-}O_2C_6H_4)_2]^{2-}$ [11].

Based on the C–O and C1–C2 bond lengths reported in Table 1, it follows that also in this case the quinoidal ligand has a catecholate nature.

The vanadyl ion is one of the very few ions able to give structurally characterised bis(quinoidal) complexes (for example, with reference to the previous titanium complexes, $[TiO(Cat)_2]^{2-}$ is dimeric) [8], even if $[VO\{1,2\text{-}O_2C_6H_2(3,5\text{-}Bu^t)_2\}_2]$ [13], for which no reversible process has been detected [12], is dimeric too.

Since in the presence of an excess of catechol, aqueous solutions of the vanadyl salt ($8 < pH < 11$) afford a reversible reduction at a mercury electrode ($E^{0\prime} = -0.72$ V versus SCE), it has been assumed that in excess of catechol the $(V^{IV}O)$bis-catecholate converts to the (V^{IV})tris-catecholate, which in turn undergoes reversible reduction to the corresponding V^{III} derivative (see below) [11].

Table 1
Selected bond lengths (in Å) for $[VO(1,2\text{-}O_2C_6H_4)_3]^{2-}$ and related bis-catecholamide species

Complex	$V\text{–}O_{(vanadyl)}$	$V\text{–}O_{(quinoid)}$	C–O	C1–C2	Counter cation	Reference
$[VO(1,2\text{-}O_2C_6H_4)_2]^{2-}$	1.62	1.96	1.35	1.40	$[K]^+$	[11]
$[VO(phencam)]^{2-}$	1.62	1.95	1.35	1.41	$[K]^+$	[14]
$[VO(bencam)]^{2-}$	1.61	1.96	1.35	1.42	$[K]^+$	[14]

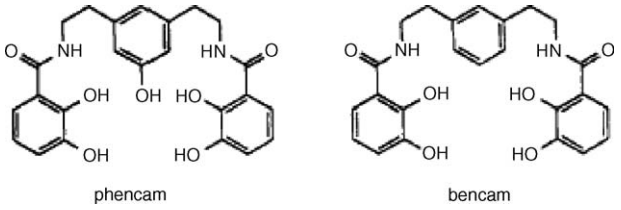

Scheme 2. Structure of a few bis-catecholamide ligands.

The square-pyramidal geometries of the dianions [VO(phencam)]$^{2-}$ and [VO(bencam)]$^{2-}$ of the bis-catecholamide ligands shown in Scheme 2 have been also structurally ascertained [14]. Also in this case the pertinent structural parameters, Table 1, support their catecholate nature.

In DMF solution, [VO(phencam)]$^{2-}$ and [VO(bencam)]$^{2-}$ display a chemically reversible (on the cyclic voltammetric time scale) one-electron oxidation ($E^{0'}$ = +0.02 and +0.03 V versus SCE, respectively), which has been arbitrarily assigned to the V(IV)/V(V) electron transfer, followed in turn by a further irreversible oxidation (E_p = +0.65 V), which has been assumed to be ligand centred [14].

2.2.1.2. Tris(quinoidal) complexes. The dianion [V(1,2-$O_2C_6H_4)_3$]$^{2-}$ possesses an almost octahedral geometry [11] similar to that illustrated in Fig. 3, which refers to the dihydroxybenzene-substituted monoanion [V{1,2-$O_2C_6H_2$(3,5-$Bu^t)_2\}_3$]$^-$ [15].

The unsubstituted dianion undergoes in MeCN solution either a chemically reversible one-electron oxidation or a one-electron reduction, which is chemically reversible only in the presence of an excess of catechol [11].

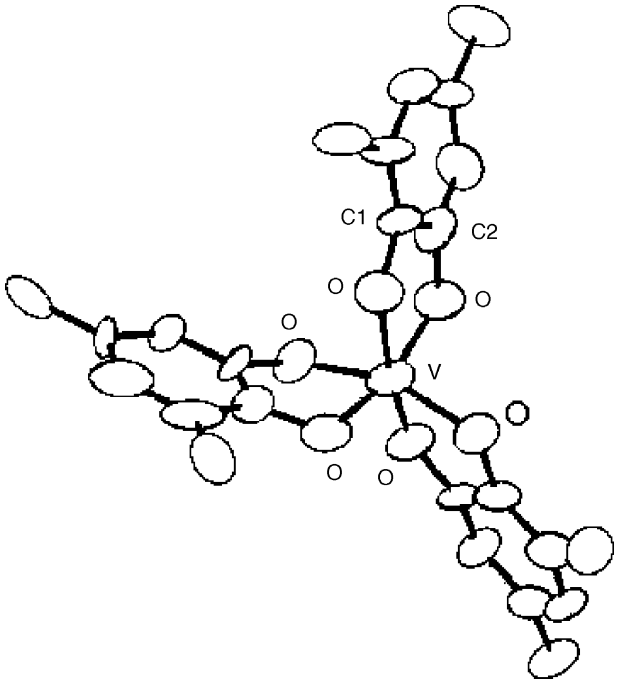

Fig. 3. X-ray crystal structure of [V{1,2-$O_2C_6H_2$(3,5-$Bu^t)_2\}_3$]$^-$. Na^+ counterion (adapted from Ref. [15]).

Table 2
Selected bond lengths (in Å) for the couple [V(1,2-$O_2C_6H_4)_3$]$^{3-/2-}$ and related species

Complex	V–O	C–O	C1–C2	α[a] (°)	Counter cation	Reference
[V(1,2-$O_2C_6H_4)_3$]$^{3-}$	2.01	1.35	1.41	45.6	$[K]^+$	[11]
[V(1,2-$O_2C_6H_4)_3$]$^{2-}$	1.94	1.34	1.41	38.9	$[Et_3NH]^+$	[11]
[V{1,2-$O_2C_6H_2$(3,5-$Bu^t)_2\}_3$]$^-$	1.91	1.34	1.41	39.0	$[Na]^+$	[15]

[a] Trigonal twist angle (see text).

The pseudooctahedral geometry of the trianion [V(1,2-$O_2C_6H_4)_3$]$^{3-}$ has been structurally ascertained [11]. A comparison of selected bond lengths for the redox couple [V(1,2-$O_2C_6H_4)_3$]$^{3-/2-}$ is compiled in Table 2.

Since in both cases the C–O and C1–C2 distances indicate a catecholate nature, it is evident that the [V(Cat)$_3$]$^{2-}$/[V(Cat)$_3$]$^{3-}$ reduction involves the V(IV)/V(III) step.

Not only are structural data unavailable for the likely stable monoanion [V(1,2-$O_2C_6H_4)_3$]$^-$, which is generated in the oxidation process, but unfortunately an EPR investigation is also lacking; this could have supported its ligand- or metal-centred nature.

As deducible from Table 2, in the case of the monoanion [V{1,2-$O_2C_6H_2$(3,5-$Bu^t)_2\}_3$]$^-$ the ligands obey the canonical criteria for the catecholate form, so that it can be described as [V^V(3,5-DBCat)$_3$]$^-$ (from hereafter: DB = di-*tert*-butyl). The progressive decrease of the V–O bond length on going from [V(Cat)$_3$]$^{3-}$ to [V(Cat)$_3$]$^{2-}$ to [V(3,5-DBCat)$_3$]$^-$ agrees with the sequential oxidation states V(III)/V(IV)/V(V).

Since it has been briefly reported that the dianion [V^{IV}(3,5-DBCat)$_3$]$^{2-}$ in MeCN solution (in the presence of free ligand) undergoes a reversible one-electron reduction to the corresponding [V^{III}(3,5-DBCat)$_3$]$^{3-}$ [11], it follows that while the conversion between the structurally uncharacterised species [V(3,5-DBCat)$_3$]$^{2-/3-}$ has been electrochemically checked, the electrochemical passage from [V(3,5-DBCat)$_3$]$^{2-}$ to the structurally defined [V(3,5-DBCat)$_3$]$^-$ is unknown.

More interesting appears the electrochemical behaviour of the tetrachloro-substituted monoanion [V(1,2-$O_2C_6Cl_4)_3$]$^-$, which based on spectroscopic data is also assigned as [V^V(Cl$_4$Cat)$_3$]$^-$ [15]. It also undergoes either a (coulometrically ascertained) one-electron oxidation or a one-electron reduction, both displaying features of chemical reversibility [15]. In the short times of cyclic voltammetry, the one-electron oxidation is assigned as a ligand centred process, but in reality the species resulting from exhaustive oxidation possesses spectroscopic features quite similar to that of the neutral species [V(1,2-$O_2C_6Cl_4)_3$], which, based on crystallographic and spectroscopic data, seems to be the semiquinonate complex [V^{III}(Cl$_4$SQ)$_3$] (from hereafter, SQ = semiquinonate) [15]. Hence an internal charge reorganisation follows the one-electron removal:

$$[V^V(Cl_4Cat)_3]^- \underset{+e}{\overset{-e}{\rightleftarrows}} [V^V(Cl_4Cat)_2(Cl_4SQ)] \rightarrow [V^{III}(Cl_4SQ)_3]$$

The one-electron reduction of the monoanion is believed to lead to the corresponding V(IV) dianion [V(Cl$_4$Cat)$_3$]$^{2-}$.

Table 3
Formal electrode potentials (V vs. SCE) for the redox processes of a few tris-quinoidal vanadium complexes in MeCN solution

Complex	$E^{0'}_{Ox}$	$E^{0'}_{Red}$	Reference
$[V^{IV}(Cat)_3]^{2-}$	−0.04 V	−0.86[a]	[11]
$[V^{V}(3,5\text{-DBCat})_3]^{-}$		−1.21[a]	[11]
$[V^{V}(Cl_4Cat)_3]^{-}$	+0.69	−0.47	[15]

[a] Chemically reversible in the presence of excess of free ligand.

Table 3 compiles the formal electrode potentials for the redox changes exhibited by until now discussed tris-quinoidal vanadium complexes.

We now pass to the topic of vanadium (and in particular of iron): polycatecholate complexes [1c].

One of the most powerful sequestering agents useful for iron transport is enterobactin (2,3-hydroxy-*N*-benzoyl-*l*-serine), a microbial tripod-like macrocyclic molecule bearing three appended catecholate (or better, catecholamide) groups [16]. Attempts to solve the crystal structure of $[Fe(ent)]^{3-}$ (from hereafter, ent = enterobactin) (see Section 2.5.1.1) have so far failed. In contrast, the pseudooctahedral geometry of the vanadium complex $[V(ent)]^{2-}$ has been determined, Fig. 4 [16] (the stability of the vanadium complex is not unexpected in view of the ability of certain marine organisms (tunicates) containing tris(pyrogallol) moieties to accumulate vanadium from sea [1c,17]).

A similar geometry is possessed by the vanadium complexes with enterobactin- or tunichrome B1-like ligands illustrated in Scheme 3.

A few significant structural data are summarized in Table 4 [16].

The V(IV) dianions undergo a one-electron oxidation, which ranges from chemically reversible to partially chemically reversible, and in some cases a one-electron reduction is also observed [16b]. Both processes have been assigned as metal-centred [16–18]. Table 5 compiles the pertinent redox potentials.

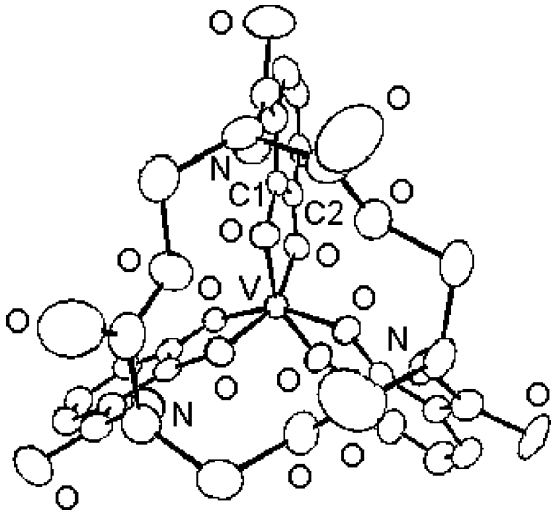

Fig. 4. X-ray crystal structure of $[V(ent)]^{2-}$. K^+ counterion (adapted from Ref. [16]).

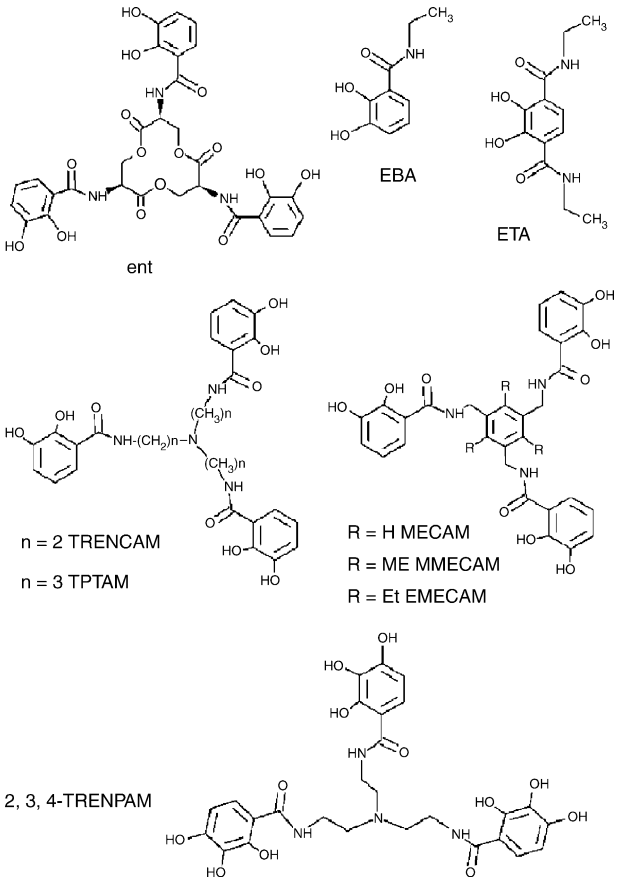

Scheme 3. Structure of enterobactin and other ligands of biological interest.

In spite of the apparent instability of the electrogenerated trianion $[V(TRENCAM)]^{3-}$ both in aqueous and non-aqueous solution, it has been successfully prepared and crystallographically characterised (Table 4). On passing we note that the C1–C2 distance would fall within the limits of the semiquinonate form, but the C–O distance is pertinent to that of catecholate form. As a matter of fact, the statistical treatment [7] affords a Δ value of −1.94, which supports the catecholate nature of the trianion, thus further confirming the metal-centred nature of the reduction process.

A further development in metal-sequestering ligands is demonstrated by the macrobicyclic tricatecholates shown in Scheme 4.

As an example, Fig. 5 shows the trigonal prismatic geometry of the vanadium complex of the (already mentioned) bicapped-TRENCAM ligand, $[V^{IV}(bicapped\text{-}TRENCAM)]^{2-}$ [9].

Table 4
Selected bond lengths (in Å) and trigonal twist angles (°) for the vanadium complexes with enterobactin and related analogues

Complex	V–O	C–O	C1–C2	α	Conter cation	Reference
$[V^{IV}(ent)]^{2-}$	1.95	1.34	1.41	28	$[K]^+$	[16a,b]
$[V^{IV}(EBA)_3]^{2-}$	1.94	1.33	1.41	36	$[K]^+$	[16b]
$[V^{III}(TRENCAM)]^{3-}$	2.00	1.33	1.46	40.8	$[K]^+$	[17]
$[V^{IV}(EMECAM)]^{2-}$	1.96	[a]	[a]	29.9	$[K]^+$	[16c]

[a] Not available.

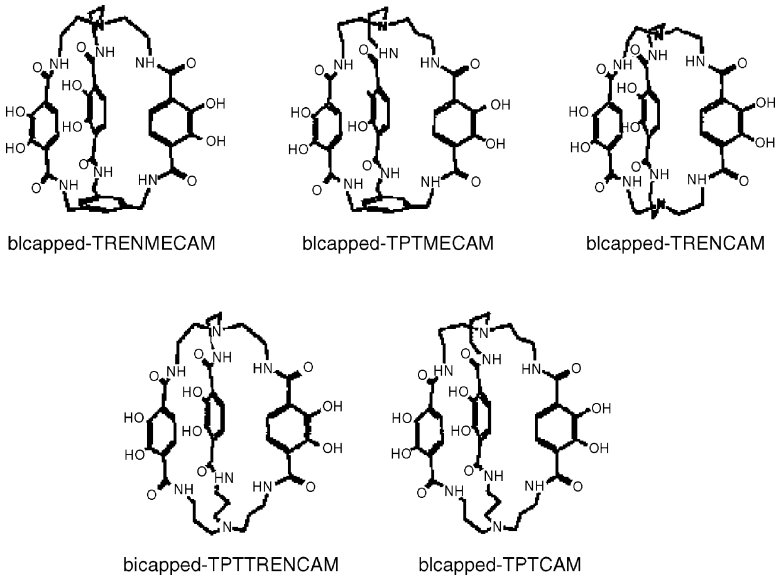

Scheme 4. Structure of a few macrobicyclic tricatecholates.

As happens for the corresponding monocapped complexes, the present metal-caged complexes undergo a metal based one-electron oxidation which ranges from chemically reversible to partially chemically reversible [18]. The respective formal electrode potentials are compiled in Table 6 [18].

Comparison with the formal electrode potentials of the corresponding monocapped derivatives shows that the bicapped complexes are more difficult to oxidise (i.e. the oxidation state V(IV) is more stable), in agreement with the less basic character of the bis-amide ligands.

2.3. Group 6 metalla-complexes (Cr, Mo, W)

2.3.1. Chromium complexes

2.3.1.1. Tris(quinoidal) complexes. Fig. 6 shows the pseudooctahedral geometry of the trianion $[Cr(1,2\text{-}O_2C_6H_4)_3]^{3-}$ [19].

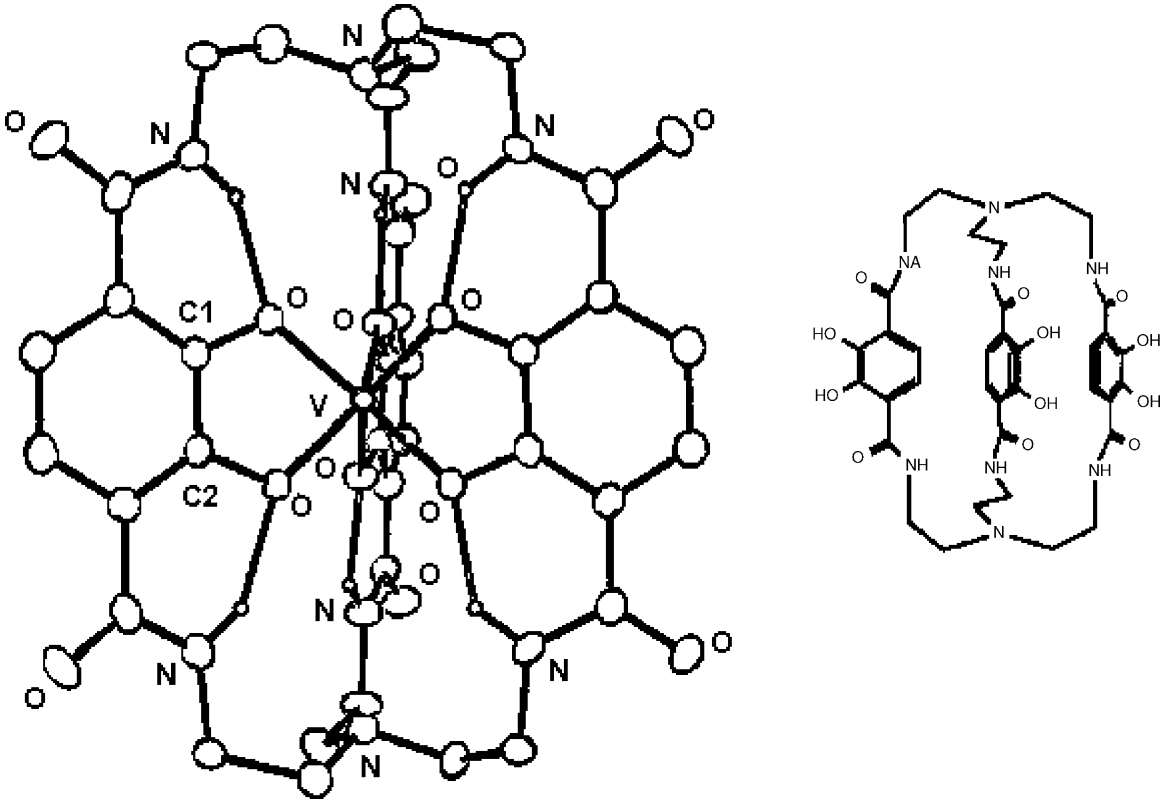

Fig. 5. X-ray crystal structure of $[V(bicapped\text{-}TRENCAM)]^{2-}$. Average bond lengths: V–O = 1.92 Å; C–O = 1.33 Å; C1–C2 = 1.41 Å; $\alpha = 11.2°$ (adapted from Ref. [9]).

Table 5
Formal electrode potentials (V vs. SCE) for the one-electron oxidation of different vanadium(IV)–polycatecholate complexes

Complex	$E^{0'}_{Ox}$	$E^{0'}_{Red}$	Solvent	Reference
$[V(ent)]^{2-}$	+0.39[a]		DMF	[16b]
$[V(EBA)_3]^{2-}$	+0.28[a]		DMF	[16b]
$[V(ETA)_3]^{2-}$	+0.72[b]		DMF	[18]
$[V(TRENCAM)]^{2-}$	+0.24[a]		DMF	[16b]
	+0.45[c]	−0.61[c]	DMF	[17]
		−0.45[c]	H_2O[d]	[17]
$[V(TPTCAM)]^{2-}$	+0.28[a]		DMF	[18]
$[V(MECAM)]^{2-}$	+0.33[c]		DMF	[16c]
$[V(MMECAM)]^{2-}$	+0.32[a]		DMF	[16c]
$[V(EMECAM)]^{2-}$	+0.33[c]		DMF	[16c]
$[V(2,3,4\text{-}TRENPAM)]^{2-}$		−0.75[c]	H_2O[d]	[17]

[a] Chemically reversible on the cyclic voltammetric time-scale.
[b] Chemically irreversible on the cyclic voltammetric time-scale.
[c] Partially chemically reversible on the cyclic voltammetric time-scale.
[d] $NaClO_4$ 0.4 mol dm^{-3}, pH 11.7.

Table 6
Formal electrode potentials for a few bicapped-polycatecholate complexes of vanadium(IV) (V vs. SCE; DMF solution)

Complex	$E^{0'}_{V(IV)/V(V)}$
$[V^{IV}(bicapped\text{-}TRENCAM)]^{2-}$	+0.67[a]
$[V^{IV}(bicapped\text{-}TPTTRENCAM)]^{2-}$	+0.64[a]
$[V^{IV}(bicapped\text{-}TPTCAM)]^{2-}$	+0.66[b]

[a] Chemically reversible on the cyclic voltammetric time-scale.
[b] Partially chemically reversible on the cyclic voltammetric time-scale.

The bond lengths (Table 7, below) are diagnostic of its catecholate nature, i.e. $[Cr^{III}(Cat)_3]^{3-}$.

In principle, with the simplification that the oxidation state of the metal does not change, tris-quinoidal complexes can undergo the following seven-membered redox sequence:

$$[M^{III}(SQ)_3]^0 \overset{+e}{\rightleftarrows} [M^{III}(SQ)_2(Cat)]^- \overset{+e}{\rightleftarrows} [M^{III}(SQ)(Cat)_2]^{2-} \overset{+e}{\rightleftarrows} [M^{III}(Cat)_3]^{3-}$$
$$\text{with } [M^{III}(SQ)_3]^0 \overset{-e}{\rightleftarrows} [M^{III}(Q)(SQ)_2]^+ \overset{-e}{\rightleftarrows} [M^{III}(Q)_2(SQ)]^{2+} \overset{-e}{\rightleftarrows} [M^{III}(Q)_3]^{3+}$$

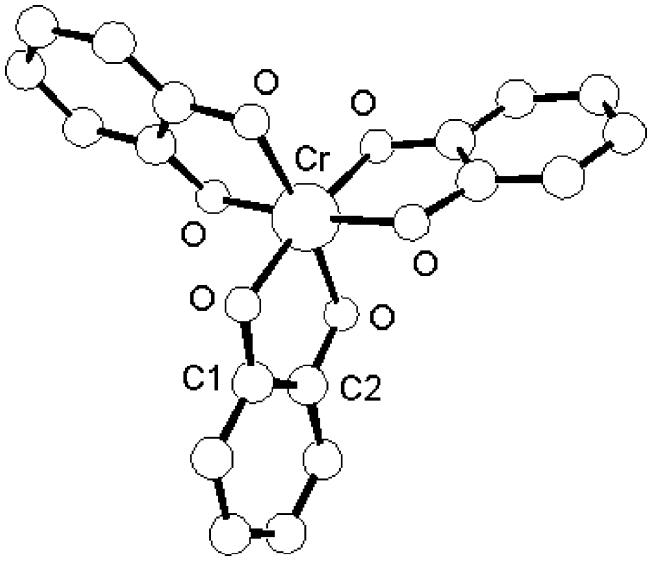

Fig. 6. X-ray crystal structure of $[Cr(1,2\text{-}O_2C_6H_4)_3]^{3-}$. K^+ countercation (adapted from Ref. [19]).

In fact, theoretical calculations on the seven-membered sequence $[Cr(1,2\text{-}O_2C_6H_4)_3]^{3+/2+/+/0/-/2-/3-}$ support the view that the charge on chromium does not change with electron additions/removals, which means that the redox changes involved are centred on the ligands [20]. As a matter of fact, electrochemical investigations have experimentally detected the sequence $[Cr(1,2\text{-}O_2C_6H_4)_3]^{3-/2-/-/0}$, Fig. 7, but X-ray absorption spectroscopic data, showing significant variations mainly in the Cr–O bond lengths, seem to indicate that the aforesaid redox changes are centred on the metal [5a].

In reality, as deducible from Table 7, some significant variations also occur at ligand level, so it cannot be ruled out that electron delocalisation might be operative.

Passing to substituted 1,2-hydroxybenzene complexes, the neutral complex $[Cr\{1,2\text{-}O_2C_6H_2(3,5\text{-}Bu^t)_2\}_3]^0$ essentially possesses an octahedral geometry ($\alpha = 50.5°$) and, based on the C–O (1.29 Å) and C1–C2 (1.43 Å) distances, it is the semiquinonate complex $[Cr^{III}(3,5\text{-}DBSQ)_3]$ [21].

The same holds for the 9,10-phenanthrensemiquinonate complex $[Cr(9,10\text{-}O_2C_{14}H_8)_3]^0$ (C–O = 1.29 Å; C1–C2 = 1.42 Å), which can be hence represented as $[Cr^{III}(PhenSQ)_3]$ [1e,22].

Table 7
Formal electrode potentials (V vs. Ag/AgCl; CH_2Cl_2 solution) and selected bond lengths (in Å) for the redox members $[Cr(1,2\text{-}O_2C_6H_4)_3]^{3-/2-/-}$

Complex	$E^{0'}_{3-/2-}$	$E^{0'}_{2-/-}$	$E^{0'}_{-/0}$	Cr–O	C–O	C1–C2	Reference
$[Cr(1,2\text{-}O_2C_6H_4)_3]^{3-}$	−0.30	−0.09	+0.40	1.98[a,b]	1.35	1.38	[5a]
				1.99[a,c]	1.35	1.40	[5a]
				1.99[d]	1.35	1.41	[19]
$[Cr(1,2\text{-}O_2C_6H_4)_3]^{2-}$				1.94[a,b]	1.32	1.37	[5a]
				1.97[a,c]	1.33	1.38	[5a]
$[Cr(1,2\text{-}O_2C_6H_4)_3]^{-}$				1.94[a,b]	1.35	1.38	[5a]
				1.95[a,c]	1.34	1.38	[5a]

[a] From XAS analysis.
[b] Ambient temperature.
[c] At 10 K.
[d] From X-ray crystallography.

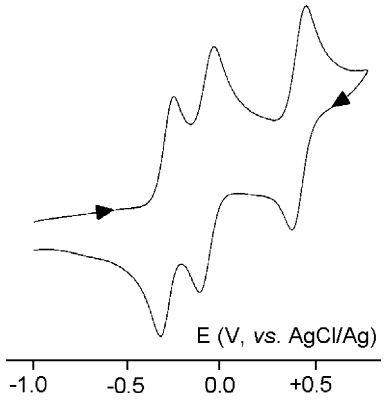

Fig. 7. Cyclic voltammogram recorded at a glassy carbon electrode in dmf solution of $[Cr^{III}(1,2\text{-}O_2C_6H_4)_3]^{3-}$. Scan rate 0.1 V s^{-1} (adapted from Ref. [5a]).

Table 8
Formal electrode potentials (V vs. SCE) for the redox processes exhibited by a few tris-quinoidal chromium complexes in CH_2Cl_2 solution

Complex	$E^{0'}_{3+/2+}$	$E^{0'}_{2+/+}$	$E^{0'}_{+/0}$	$E^{0'}_{0/-}$	$E^{0'}_{-/2-}$	$E^{0'}_{2-/3-}$
$[Cr(3,5\text{-}DBSQ)_3]^0$		+1.22	+1.00	−0.21	−0.72	−1.29
$[Cr(PhenSQ)_3]^0$	+1.15	+1.01	+0.82	−0.15	−0.48	−0.91
$[Cr(Cl_4SQ)_3]^0$				+0.82	+0.44	0.00
$[Cr(Br_4SQ)_3]^0$				+0.83	+0.43	+0.17

In agreement with the sequence of redox changes which can be potentially exhibited by tris-quinoidal complexes, $[Cr^{III}(3,5\text{-}DBSQ)_3]$ exhibits three stepwise one-electron reduction processes and two stepwise one-electron oxidation processes in CH_2Cl_2 solution, all exhibiting features of chemical reversibility, Fig. 8 [23].

Rich redox behaviour is displayed also by both $[Cr(PhenSQ)_3]^0$ [23] and $[Cr(X_4SQ)_3]^0$ (X = Cl [23], Br [24]), Table 8.

Structural data from X-ray absorption spectroscopy in conjunction with EPR spectroscopy for the monoanion $[Cr\{1,2\text{-}O_2C_6H_2(3,5\text{-}Bu^t)_2\}_3]^-$ have been interpreted in the sense of $[Cr^V(3,5\text{-}DBCat)_3]^-$ metal/ligand oxidation states [5b], an interpretation which has been contested in favor of $[Cr^{III}(3,5\text{-}DBSQ)_2(3,5\text{-}DBCat)]^-$ [25]. In this context, Table 9 summarizes a few selected data pertinent to the redox couple.

As a matter of fact, both the C–O and C1–C2 distances in the monoanion seem to obey the statistical criteria for the (partial) semiquinonate nature of the ligands. In addition, the statistical treatment [7] gives a Δ value of −1.09, which also seems to support the semiquinonate nature.

Table 9
Selected bond lengths (in Å) for the couple $[Cr\{1,2\text{-}O_2C_6H_2(3,5\text{-}Bu^t)_2\}_3]^{0/-}$

Complex	Cr–O	C–O	C1–C2	α (°)	Counter cation	Reference
$[Cr\{1,2\text{-}O_2C_6H_2(3,5\text{-}Bu^t)_2\}_3]^0$	1.93	1.29	1.43	48.6		[21]
$[Cr\{1,2\text{-}O_2C_6H_2(3,5\text{-}Bu^t)_2\}_3]^-$	1.96	1.28	1.46	≈50	$[K]^+$	[5b]

Table 10
Average bond lengths (Å) in the series $[Cr(1,2\text{-}O_2C_6Cl_4)_3]^0/[Cr(1,2\text{-}O_2C_6Cl_4)_3]^-/[Cr(1,2\text{-}O_2C_6Cl_4)_3]^{2-}$ and $[Cr(1,2\text{-}O_2C_6Br_4)_3]^-/[Cr(1,2\text{-}O_2C_6Br_4)_3]^{2-}$

Complex	Cr–O	C–O	C1–C2
$[Cr(1,2\text{-}O_2C_6Cl_4)_3]^0$	1.95	1.28	1.40
$[Cr(1,2\text{-}O_2C_6Cl_4)_3]^-$	1.94	1.30	1.40
$[Cr(1,2\text{-}O_2C_6Cl_4)_3]^{2-}$	1.96	1.30	1.40
$[Cr(1,2\text{-}O_2C_6Br_4)_3]^-$	1.94	1.30	1.40
$[Cr(1,2\text{-}O_2C_6Br_4)_3]^{2-}$	1.94	1.32	1.40

Complete sets of structural data are also available for the redox sequences exhibited by $[Cr(1,2\text{-}O_2C_6X_4)_3]^0$ (X = Cl, Br) [24,26,27]. Based on the cited assumption that the neutral complex would correspond to $[Cr^{III}(X_4SQ)_3]$, the related anions should be represented as $[Cr^{III}(X_4SQ)_2(X_4Cat)]^-$, $[Cr^{III}(X_4SQ)(X_4Cat)_2]^{2-}$ and $[Cr^{III}(X_4Cat)_3]^{3-}$, respectively.

As deducible from Table 10, the variations in bond lengths following the redox changes are minimal, in particular as far as the Cr–O and C1–C2 distances are concerned. From a speculative viewpoint, a significant elongation (by about 0.2 Å) can be found in the C–O distance on passing from the neutral to the anionic species.

This result supports the ligand-centred nature of the electron addition. Further, the homogeneity in the distances inside the three reduced ligands suggest a delocalisation of the added electrons over the three centres (in agreement with the fact that separate redox changes indicate charge delocalisation in mixed-valent species) [4]. The substantial invariance of the Cr–O distances seems to rule out changes in the oxidation state of the central metal.

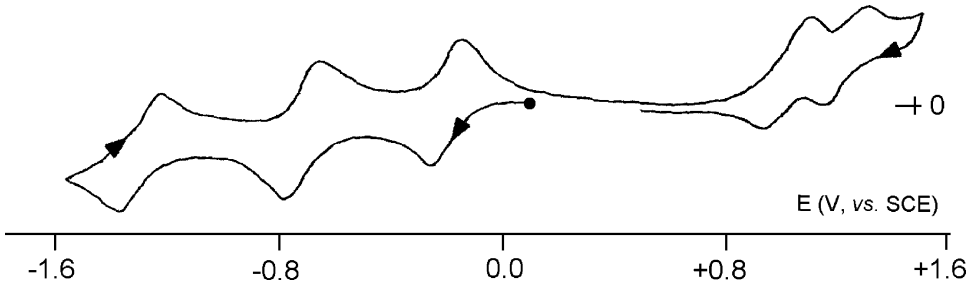

Fig. 8. Cyclic voltammogram recorded at a platinum electrode in MeCN solution of $[Cr^{III}(3,5\text{-}DBSQ)_3]$. Scan rate 0.05 V s^{-1} (adapted from Ref. [23]).

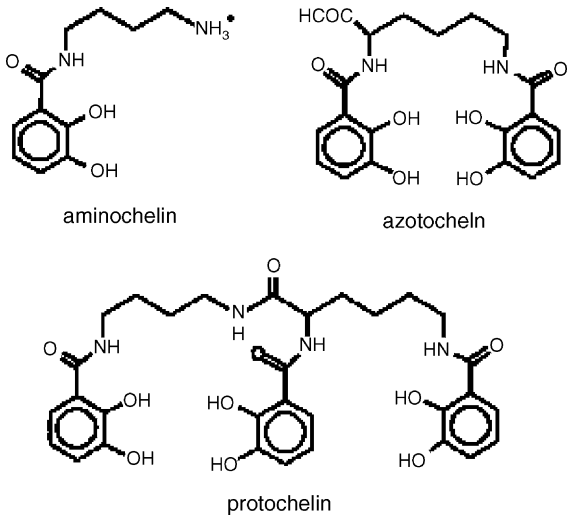

Scheme 5. Structure of a few polycatecholate ligands able to act as siderophores.

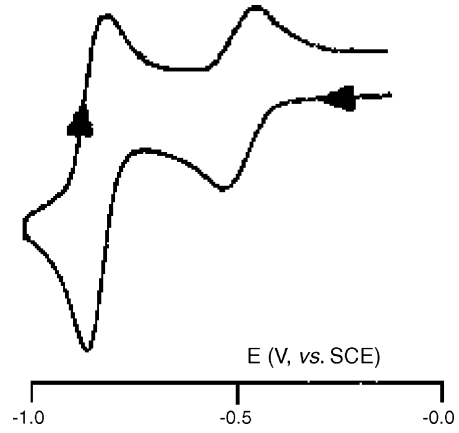

Fig. 10. Cyclic voltammogram recorded in aqueous solution (pyridine buffer, pH 6.6) of $[MoO_2(Cat)_2]^{2-}$. Scan rate 0.2 V s^{-1} (adapted from Ref. [32]).

2.3.2. Molybdenum complexes

Molybdenum is a powerful competitor of iron in the affinity for catecholamide-based chelators, so that research has addressed not only common catecholate ligands, but also catecholamide chelators, in particular those polycatecholate molecules which mimic siderophores from *Azotobacter vinelandii*, Scheme 5 [28].

2.3.2.1. Bis(quinoidal) complexes. A series of bis(quinoidal) oxo-molybdenum complexes is structurally known. In fact, both the square pyramidal geometry of the monooxo monoanion $[MoO\{1,2\text{-}O_2C_6H_2(3,6\text{-}Bu^t)_2\}_2]^-$ [29], and the distorted octahedral geometry of the *cis*-dioxo dianions $[MoO_2(1,2\text{-}O_2C_6H_4)_2]^{2-}$ [30], $[MoO_2\{1,2\text{-}O_2C_6H_3(COOH)\}_2]^{2-}$ [31], $[MoO_2(BAX)]^{2-}$ (BAX = tetradeprotonated α,α'-bis(2,3-dihydroxybenzoylamino)-*m*-xylene tetranion) [28b] have been solved.

Fig. 9 representatively shows the molecular structures of $[MoO\{1,2\text{-}O_2C_6H_2(3,6\text{-}Bu^t)_2\}_2]^-$ and $[MoO_2\{1,2\text{-}O_2C_6H_3(COOH)\}_2]^{2-}$, respectively.

As deduced from Table 11, the structural parameters indicate the catecholate nature of the ligands in all the complexes.

The reduction paths exhibited by $[Mo^{VI}O_2(Cat)_2]^{2-}$ have been accurately studied in aqueous solution [32]. As shown in Fig. 10, at pH 6.6 it undergoes a one-electron addition ($E^{0'} = -0.48$ V versus SCE) followed in turn by a two-electron addition ($E^{0'} = -0.83$ V).

Such processes have been assigned to the reversible (on the cyclic voltammetric time scale) sequence Mo(VI)/

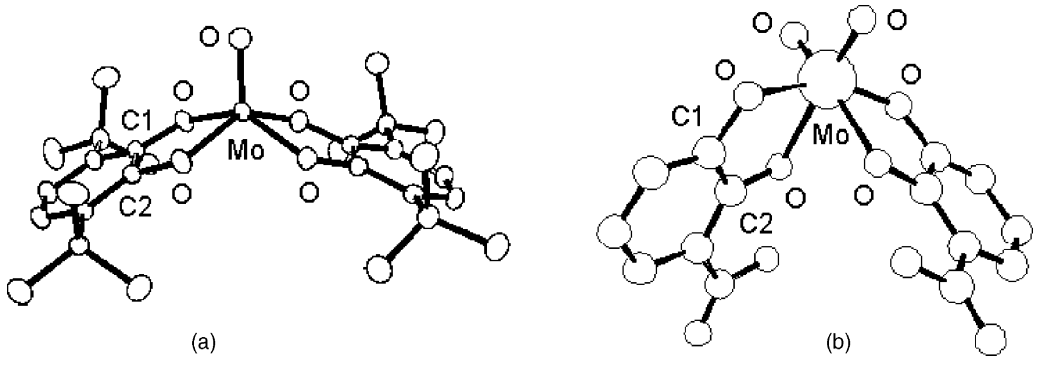

Fig. 9. X-ray crystal structures of: (a) $[MoO\{1,2\text{-}O_2C_6H_2(3,6\text{-}Bu^t)_2\}_2]^-$; (b) $[MoO_2\{1,2\text{-}O_2C_6H_3(COOH)\}_2]^{2-}$ (adapted from Refs. [29,31], respectively).

Table 11
Selected structural data (average bond lengths in Å) for a few bis-quinoidal dioxo-molybdenum complexes

Complex	Mo–$O_{(oxo)}$	Mo–$O_{(quin)}$	C–O	C1–C2	Counterion	Reference
$[MoO\{1,2\text{-}O_2C_6H_2(3,6\text{-}Bu^t)_2\}_2]^-$	1.69	1.98	1.37	1.40	$[Co(C_5H_5)_2]^+$	[29]
$[MoO_2(1,2\text{-}O_2C_6H_4)_2]^{2-}$	1.77	2.10	1.39	1.41	$[K]^+$	[30a]
$[MoO_2\{1,2\text{-}O_2C_6H_3(COOH)\}_2]^{2-}$	1.71	2.08	1.34	1.41	$[NMe_4]^+$	[31]
$[MoO_2(BAX)]^{2-}$	1.72	2.08	1.34	1.41	$[Na]^+$	[28b]

Table 12
Formal electrode potentials (V vs. AgCl/Ag) for the reduction processes exhibited by dioxomolybdenum-catecholates in aqueous solution (pH 6.7)

Complex	$E^{0'}_{Mo(VI)/Mo(V)}$	$E^{0'}_{Mo(V)/Mo(III)}$	Reference
$[MoO_2(Cat)_2]^{2-}$	−0.51	−0.85	[32]
$[MoO_2(aminochelin)_2]^{2-}$	−0.52	−0.81	[28c]
$[MoO_2(azotochelin)]^{2-}$	−0.42	−0.78	[28c]
$[MoO_2(protochelin)]^{2-}$	−0.41	−0.75	[28c]

Mo(V)/Mo(III). As expected, the response is affected both by pH and the coordinating properties of the buffer, so it would deserve investigation in non-aqueous solvent to assess the intrinsic electron-transfer ability not only of the central Mo(VI) ion but also of the catechol ligands.

Quite similar behaviour is exhibited by complexes with the siderophores illustrated in Scheme 5 [28c]; Table 12 compiles the respective formal electrode potentials.

The crystal structure of $[MoO_2(H_2\text{-bicapped-TRENCAM})]^{2-}$ is known. Only two of the three catecholamide subunits are coordinated [18].

2.3.2.2. Comparison with the bis-dithiolene analogs. Selected structural data for the octahedral dianions $[Mo^{VI}O_2(1,2\text{-}O_2C_6H_4)_2]^{2-}$ and $[Mo^{VI}O_2(1,2\text{-}S_2C_6H_4)_2]^{2-}$ are reported in Table 13.

In contrast with $[Mo^{VI}O_2(1,2\text{-}O_2C_6H_4)_2]^{2-}$, $[Mo^{VI}O_2(1,2\text{-}S_2C_6H_4)_2]^{2-}$ undergoes in DMF solution either an irreversible oxidation ($E_p = +0.04$ V versus SCE) or an irreversible reduction ($E_p = -0.97$ V) [33], pointing to the instability of both the Mo(VI)-dithione monoanion and the Mo(V)-dithiolate oxidation states.

2.3.2.3. Tris(quinoidal) complexes. The trigonal prismatic derivative $[Mo(9,10\text{-}O_2C_{14}H_8)_3]$ is the only example of a structurally characterised tris(quinoidal)-mononuclear complex of molybdenum [34]. In it, two phenanthrene quinoidal subunits are planar and exhibit bond lengths approaching catecholate nature (C–O = 1.35 Å; C1–C2 = 1.35 Å; Mo–O = 1.95 Å), whereas the third subunit is bent and exhibits bond lengths approaching semiquinone character (C–O = 1.31 Å; C1–C2 = 1.43 Å; Mo–O = 1.98 Å). On this basis, the complex has been assigned as $[Mo^{V}(PhenCat)_2(PhenSQ)]$.

2.3.3. Tungsten complexes

2.3.3.1. Tris(quinoidal) complexes. Electrochemical information on $[W^{VI}(3,5\text{-DBCat})_3]^0$ has been reported (two sequential one-electron reduction processes) [35], but no structural data are available.

Table 14
Selected structural data (average bond lengths in Å; twist angles in °) for a few tris-quinoidal manganese complexes

Complex	Mn–O	C–O	C1–C2	α	Counter cation	Reference
$[Mn\{1,2\text{-}O_2C_6H_2(3,5\text{-}Bu^t)_2\}_3]^{2-}$	1.91	1.36	1.40	51.8	$[K]^+$	[37a,c]
	1.88	1.34	1.40		$[Na]^+$	[37b]
$[Mn\{1,2\text{-}O_2C_6H_2(3,6\text{-}Bu^t)_2\}_3]^0$	1.92[a]	1.28[a]	1.45[a]	52.5		[38]
	1.88[b]	1.31[b]	1.44[b]			
	1.87[c]	1.31[b]	1.42[c]			
$[Mn(1,2\text{-}O_2C_6Cl_4)_3]^{2-}$	1.89	1.32	1.39	53.9	$[PPh_4]^+$	[39]
	1.91	1.33	1.38	≈54	$[NBu_4]^+$	[40]

[a] First subunit.
[b] Second subunit.
[c] Third subunit.

2.4. Group 7 metalla complexes (Mn, Tc, Re)

2.4.1. Manganese complexes

2.4.1.1. Bis(quinoidal) complexes. The bis-complex of 1,2-dihydroxybenzene-3,5-disulfonate (Tiron) $[Mn\{1,2\text{-}O_2C_6H_2(3,5\text{-}SO_3)_2\}_2]^{5-}$ has been structurally characterised [36]. The relevant C–O and C1–C2 distances (1.36 and 1.41 Å, respectively) support the catecholate nature of the ligands, so that the pentaanion can be represented as $[Mn^{III}\{(3,5\text{-}SO_3)_2Cat\}_2]^{5-}$.

2.4.1.2. Tris(quinoidal) complexes. The essentially octahedral geometries of the dianion $[Mn\{1,2\text{-}O_2C_6H_2(3,5\text{-}Bu^t)_2\}_3]^{2-}$ and the neutral $[Mn\{1,2\text{-}O_2C_6H_2(3,6\text{-}Bu^t)_2\}_3]^0$ are illustrated in Fig. 11 [37,38].

A similar geometry is displayed by the dianion $[Mn(1,2\text{-}O_2C_6Cl_4)_3]^{2-}$ [39,40]. Table 14 summarizes a few selected structural parameters of the three complexes.

As far as the dianions are concerned, since the EPR results and the Mn–O bond lengths support the Mn(IV) assignment, and the C–O distances agree with a catecholate form of the dioxolene ligands, they are assigned as $[Mn^{IV}(3,5\text{-DBCat})_3]^{2-}$, and $[Mn^{IV}(Cl_4Cat)_3]^{2-}$, respectively.

In turn, analysis of bond lengths of the three subunits of the neutral complex, together with Mn–O distances, suggest a $[Mn^{IV}(3,6\text{-DBSQ})_2(3,6\text{-DBCat})]$ formulation.

In connection with the Mn(IV) oxidation state, the difficulty of Mn(III) to form tris(quinoidal) complexes has been pointed out [37a,c] (due to the short bite distance of dioxo atoms with respect to the Mn–O length, which hinders formation of octahedral coordination). In fact, the only Mn(III) homoleptic

Table 13
Structural comparison (average bond lengths in Å) between isostructural dioxolene (X = O) and dithiolene (X = S) dioxomolybdenum homologues

Complex	$Mo\text{–}O_{(dioxo)}$	Mo–X	C–X	C1–C2	Counterion	Reference
$[MoO_2(1,2\text{-}O_2C_6H_4)_2]^{2-}$	1.77	2.10	1.39	1.41	$[K]^+$	[30a]
$[MoO_2(1,2\text{-}S_2C_6H_4)_2]^{2-}$	1.71	2.51	1.74	1.37	$[NEt_4]^+$	[33]

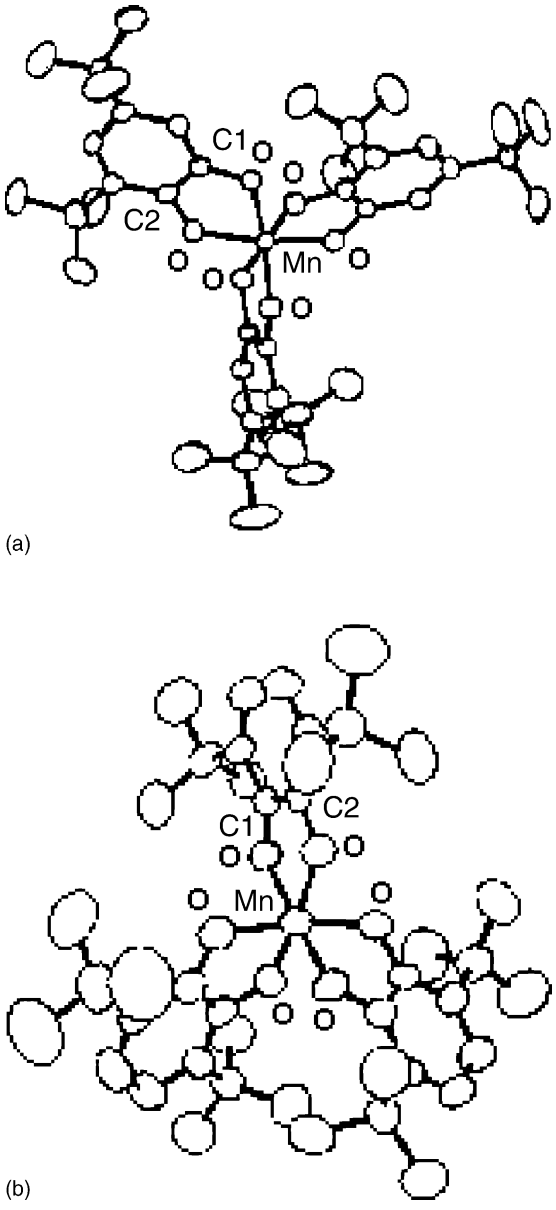

Fig. 11. X-ray crystal structures of: (a) $[Mn\{1,2\text{-}O_2C_6H_2(3,5\text{-}Bu^t)_2\}_3]^{2-}$; (b) $[Mn\{1,2\text{-}O_2C_6H_2(3,6\text{-}Bu^t)_2\}_3]^0$ (adapted from Refs. [31,32], respectively).

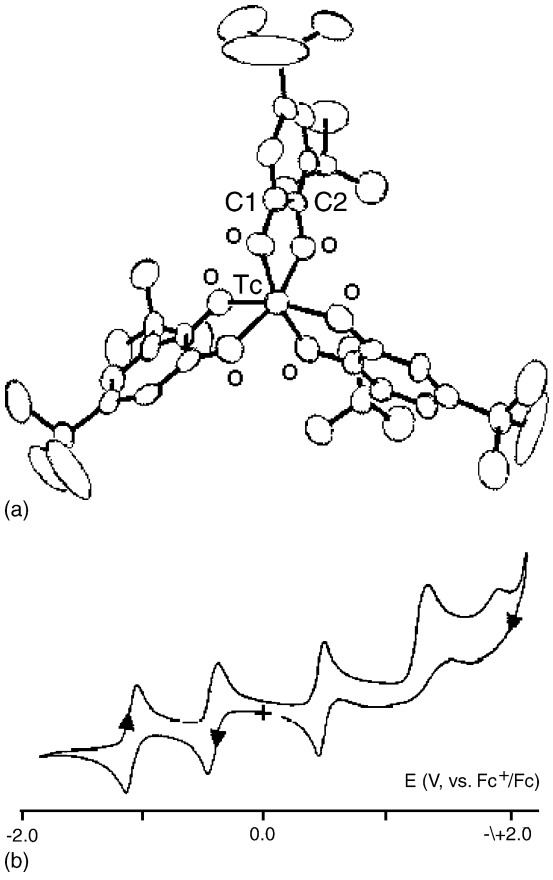

Fig. 12. (a) X-ray crystal structure of $[Tc\{1,2\text{-}O_2C_6H_2(3,5\text{-}Bu^t)_2\}_3]^0$ and (b) its cyclic voltammetric profile at a platinum electrode (in CH_2Cl_2 solution; scan rate 0.2 V s^{-1}). Average bond lengths: Tc–O = 1.95 Å; C–O = 1.34 Å; C1–C2 = 1.39 Å (adapted from Ref. [45]).

complex structurally characterised seems to be the above cited bis-catecholate complex $[Mn^{III}\{(3,5\text{-}SO_3)_2Cat\}_2]^{5-}$.

In these circumstances, it is not unexpected that no clear picture on the redox ability of $[Mn^{IV}(3,5\text{-DBCat})_3]^{2-}$ has been gained [37,41,42].

2.4.2. Technetium complexes

2.4.2.1. Bis(quinoidal) complexes. The crystal structure of the square pyramidal monoanion $[TcO(1,2\text{-}O_2C_6H_4)_2]^-$ is known [43]. The C–O (1.36 Å) and C1–C2 (1.38 Å) distances indicate the catecholate nature of the ligands. No pertinent electrochemical data are available.

2.4.2.2. Comparison with the bis-dithiolene analogue. The structural parameters of the monoanions $[TcO(1,2\text{-}O_2C_6H_4)_2]^-$ [43] and $[TcO(1,2\text{-}S_2C_6H_4)_2]^-$ [44] are compared in Table 15.

2.4.2.3. Tris(quinoidal) complexes. Fig. 12 shows the octahedral geometry of $[Tc\{1,2\text{-}O_2C_6H_2(3,5\text{-}Bu^t)_2\}_3]^0$ together with its cyclic voltammetric profile in CH_2Cl_2 solution [45]. The structural parameters confirm the catecholate nature of the ligands.

$[Tc^{VI}(3,5\text{-DBCat})_3]^0$ undergoes two chemically reversible one-electron reduction processes, which are assigned as $[Tc^{VI}(3,5\text{-DBCat})_3]^0/[Tc^{V}(3,5\text{-DBCat})_3]^-$ ($E^{0'} = -0.03$ V versus SCE) and $[Tc^{V}(3,5\text{-DBCat})_3]^-/[Tc^{IV}(3,5\text{-DBCat})_3]^{2-}$

Table 15
Structural comparison (average bond lengths in Å) between isostructural dioxolene (X = O) and dithiolene (X = S) oxotechnetium homologues

Complex	Tc=O	Tc–X	C–X	C1–C2	Counterion	Reference
$[Tc^{V}O(1,2\text{-}O_2C_6H_4)_2]^-$	1.65	1.96	1.36	1.38	$[NBu_4]^+$	[43]
$[Tc^{V}O(1,2\text{-}S_2C_6H_4)_2]^-$	1.66	2.32	1.77	1.39	$[AsPh_4]^+$	[44]

Table 16
Average bond lengths (Å) and electrochemical data (CH_2Cl_2 solution; potential values in V vs. Fc/Fc^+) for $[M^{VI}(XCat)_3]^0$ (M = Re, Tc; X = 3,5-DB, Cl_4)

M	XCat	Re–O	C–O	C1–C2	$E^{0'}_{Ox}$	$E^{0'}_{1st\ Red}$	$E^{0'}_{2nd\ Red}$	Reference
Tc	3,5-DBCat	1.95	1.34	1.39	+0.45[a]	−0.42[a]	−1.09[a]	[45]
Re	3,5-DBCat	1.93	1.35	1.38	+0.63[b]	−0.62[a]		[46]
Re	Cl_4Cat	1.94	1.34	1.38	+0.94[a]	+0.36[a]	−0.59[a]	[46]

[a] Chemically reversible.
[b] Partial chemical reversibility.

($E^{0'} = -0.70$ V), respectively, and a chemically reversible one-electron oxidation ($E^{0'} = +0.84$ V), which is assigned as $[Tc^{VI}(3,5\text{-DBCat})_3]^0/[Tc^{VI}(3,5\text{-DBCat})_2(3,5\text{-DBSQ})]^+$. A further, ligand-centred, irreversible oxidation is also present ($E_p = +1.72$ V) [45].

2.4.3. Rhenium complexes

2.4.3.1. Tris(quinoidal) complexes. $[Re\{1,2\text{-}O_2C_6H_2(3,5\text{-}Bu^t)_2\}_3]^0$ is isostructural with $[Tc^{VI}(3,5\text{-DBCat})_3]^0$ (pseudo-octahedral geometry; trigonal twist angle $\alpha = 37.9°$) [46]. The same geometry is exhibited by $[Re(1,2\text{-}O_2C_6Cl_4)_3]^0$ (trigonal twist angle $\alpha = 40.0°$) [46b].

Similarly to $[Tc^{VI}(3,5\text{-DBCat})_3]^0$, $[Re^{VI}(3,5\text{-DBCat})_3]^0$ and $[Re^{VI}(Cl_4Cat)_3]^0$ in CH_2Cl_2 solution undergo sequential one-electron transfers [46b]. Table 16 summarizes both the structural and electrochemical features, also in comparison with those of $[Tc^{VI}(3,5\text{-DBCat})_3]^0$.

As previously discussed, given the catecholate nature of the ligands, the reduction processes are assigned as metal-centred ($M^{VI}/M^{V}/M^{IV}$), whereas the oxidation process would lead to $[M^{VI}(3,5\text{-DBCat})_2(3,5\text{-DBSQ})]^+$.

2.5. Group 8 metalla-complexes (Fe, Ru, Os)

2.5.1. Iron complexes

Studies of the coordination chemistry of catechols originated from attempts to understand the nature and the functions of iron chelators (siderophores) in biology, which unfailingly contain catecholate functionalities (or better, catecholamide groups) [1,28].

2.5.1.1. Tris(quinoidal) complexes. The trianion $[Fe(1,2\text{-}O_2C_6H_4)_3]^{3-}$, which is isostructural with $[Cr(Cat)_3]^{3-}$, possesses a distorted octahedral geometry and can be represented as $[Fe^{III}(Cat)_3]^{3-}$ (see below) [19]. The crystal structures of a number of neutral tris-quinoidal complexes are known, namely: $[Fe\{1,2\text{-}O_2C_6H_2(3,5\text{-}Bu^t)_2\}_3]^0$ [47], $[Fe\{1,2\text{-}O_2C_6H_2(3,6\text{-}Bu^t)_2\}_3]^0$ [48], $[Fe(9,10\text{-}O_2C_{14}H_8)_3]^0$ [49]. Fig. 13 representatively shows the distorted octahedral geometry of $[Fe\{1,2\text{-}O_2C_6H_2(3,6\text{-}Bu^t)_2\}_3]^0$ [48]. Selected structural data are compiled in Table 17.

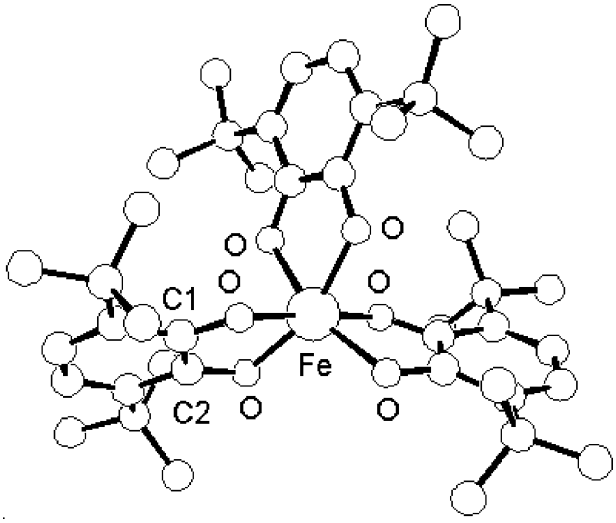

Fig. 13. X-ray crystal structure of $[Fe\{1,2\text{-}O_2C_6H_2(3,6\text{-}Bu^t)_2\}_3]^0$ (adapted from Ref. [48]).

It is quite evident that in the neutral complexes the ligands are in the semiquinonate form (or, $[Fe(3,5\text{-DBSQ})_3]^0$, $[Fe(3,6\text{-DBSQ})_3]^0$, $[Fe(phenSQ)_3]^0$, respectively), whereas, as anticipated, in the trianions they are in the catecholate form (the *N*,*N*′-diethylterephthalamide ligand is one of the precursors used to mimic enterobactin, see below).

Both $[Fe(3,5\text{-DBSQ})_3]^0$ and $[Fe(phenSQ)_3]^0$ only exhibit irreversible reduction processes [49]. The electrochemical investigation on the not readily characterized iron complexes of $1,2\text{-}O_2C_6H_2(3,5\text{-}Bu^t)_2$ has been also reported [50]. As illustrated in Fig. 14, $[Fe(3,6\text{-DBSQ})_3]^0$ exhibits the expected semiquinonate redox processes; it displays three sequential oxidation processes (only the first being chemically reversible) and three sequential

Table 17
Selected structural data (average bond lengths in Å; twist angles in °) for a few tris-quinoidal iron complexes

Complex	Fe–O	C–O	C1–C2	α	Reference
$[Fe\{1,2\text{-}O_2C_6H_2(3,5\text{-}Bu^t)_2\}_3]^0$	2.02	1.28	1.45	≈40	[47]
$[Fe\{1,2\text{-}O_2C_6H_2(3,6\text{-}Bu^t)_2\}_3]^0$	2.00	1.28	1.46	43.1	[48]
$[Fe(9,10\text{-}O_2C_{14}H_8)_3]^0$	2.03	1.28	1.44	≈46	[49]
$[Fe(1,2\text{-}O_2C_6H_4)_3]^{3-}$	2.02	1.35	1.41	44.7	[19]
$[Fe\{1,4\text{-}C(O)N(H)C_2H_5\text{-}2,3\text{-}O_2C_6H_4\}_3]^{3-}$[a]	2.03	1.32	1.42	40.0	[9]

[a] *N*,*N*′-Diethylterephthalamide ligand.

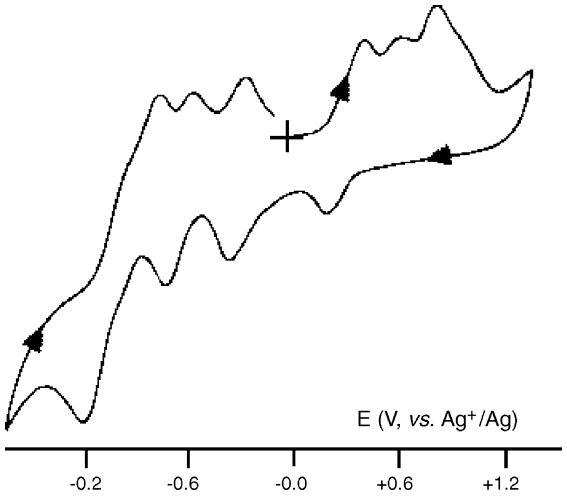

Fig. 14. Cyclic voltammogram recorded in CH_2Cl_2 solution of [Fe(3,6-DBSQ)$_3$]^0. [NBu$_4$][PF$_6$] supporting electrolyte. Scan rate 0.1 V s^{-1} (adapted from Ref. [48]).

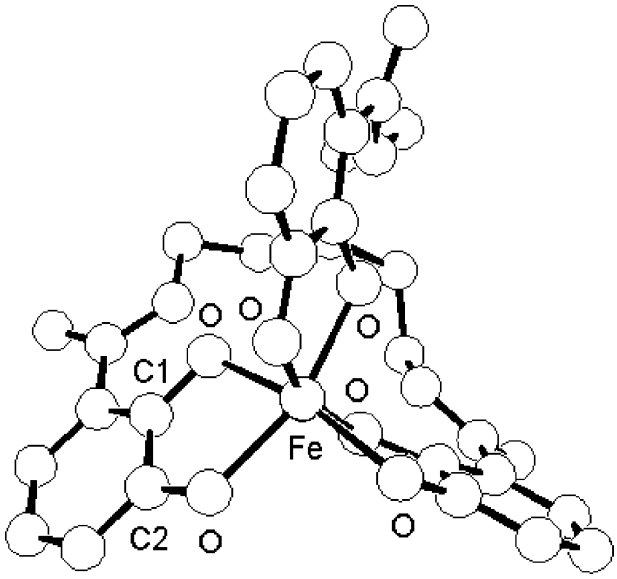

Fig. 15. X-ray crystal structure of [Fe(TRENCAM)]$^{3-}$. Fe–O = 2.01 Å; C–O = 1.32 Å; C1–C2 = 1.42 Å; α = 37.4° (adapted from Ref. [53a]).

reversible reduction processes (the last of which is almost completely overlapped by the Fe(III)/Fe(II) process) [48].

The (X-ray not characterised) trianion [Fe^{III}(Cl$_4$Cat)$_3$]$^{3-}$ in dichloromethane solution exhibits the stepwise oxidation [Fe(Cl$_4$Cat)$_3$]$^{3-/2-/-/0}$, which is clearly ligand centred, whereas in acetonitrile solution the Fe$^{III/II}$ reduction [Fe^{III}(Cl$_4$Cat)$_3$]$^{3-/4-}$ is also detected [51]. Table 18 summarizes the formal electrode potentials for the electron-transfer sequences of the two complexes.

Among biological chelators, enterobactin possesses the highest affinity for iron(III) ($K_{Fe(ent)} \approx 10^{52}$) [52]. As previously pointed out, the crystal structure of [Fe^{III}(ent)]$^{3-}$ has been not yet solved, but its electrochemical behaviour is known [52]. In aqueous solution, it undergoes the chemically reversible Fe(III)/Fe(II) reduction, the redox potential of which varies with pH, thus indicating that the electron transfer is coupled to protonation processes.

As in the case of vanadium complexes, Section 2.2.1.2, many iron(III) complexes with enterobactin-mimetic ligands (see Scheme 3) have been prepared. This is the case of [Fe(TRENCAM)]$^{3-}$, the X-ray structure of which has been solved, Fig. 15 [53a].

Like [Fe^{III}(ent)]$^{3-}$, in aqueous solution, it undergoes the reversible Fe(III)/Fe(II) reduction coupled to ligand protonation [53b]. The same behavior is displayed by iron(III) complexes of related ligands. Table 19 summarizes the pertinent electrochemical data, together with those of the bicapped analogues, which will be discussed later.

Table 19
Electrochemical data for iron-polycatecholate complexes mimetic of enterobactin (V vs. SCE; aqueous solution, pH ≈11)

Complex	$E^{0'}_{Fe(III)/Fe(II)}$	Reference
[Fe^{III}(ent)]$^{3-}$	−1.23	[52]
[Fe^{III}(TRENCAM)]$^{3-}$	−1.31	[53]
[Fe^{III}(EMECAM)]$^{3-}$	−1.34	[18c]
[Fe^{III}(MECAM)]$^{3-}$	−1.34	[18c]
[Fe^{III}(MMECAM)]$^{3-}$	−1.35	[18c]
[Fe^{III}(TPTCAM)]$^{3-}$	−1.25	[54]
[Fe^{III}(bicapped-TRENCAM)]$^{3-}$	−1.24	[54]
[Fe^{III}(bicapped-TPTCAM)]$^{3-}$	−1.19	[54]
[Fe^{III}(bicapped-TPTTRENCAM)]$^{3-}$	−1.17	[54]
[Fe^{III}(bicapped-TRENMECAM)]$^{3-}$	−1.17	[54]
[Fe^{III}(bicapped-TPTMECAM)]$^{3-}$	−1.16	[54]

The rather negative potential value for the Fe(III) reduction of the enterobactin complex (at pH 7, a $E^{0'}$ value of −1.01 V has been estimated) (as well as that of its synthetic analogues) seems to justify that, under physiological bacterial conditions, release of iron needs hydrolysis of the complex, in that the formal electrode potential is well beyond the reducing power of any in vivo reductants [52].

Table 18
Electrochemical data for a few tris-quinoidal iron complexes in non-aqueous solution

Complex	$E^{0'}_{0/-}$	$E^{0'}_{-/2-}$	$E^{0'}_{2-/3-}$	$E^{0'}_{3-/4-}$	Solvent	Reference
[Fe(Cl$_4$Cat)$_3$]$^{3-}$	+1.10[a]	+0.76[a]	+0.37[a]		CH_2Cl_2	[51]
				−1.66[a]	MeCN	[51]
[Fe(3,6-DBSQ)$_3$]^0	−0.34[b]	−0.66[b]	−0.88[b]	−1.2[b]	CH_2Cl_2	[48]

[a] Potential values (in V) vs. AgI/Ag.
[b] V vs. Ag$^+$/Ag.

As in the case of vanadium complexes, Section 2.2.1.2, the macrobicyclic polycatecholate ligands shown in Scheme 4 have been used to complex iron [54]. The molecular structure of $[Fe^{III}(bicapped\text{-}TRENCAM)]^{3-}$ is qualitatively similar to that of $[V^{IV}(bicapped\text{-}TRENCAM)]^{2-}$ illustrated in Fig. 5 (Fe–O = 2.01 Å; C–O = 1.33 Å; C1–C2 = 1.44 Å; $\alpha = 0.0°$) [54]. The same structural features are displayed by $[Fe^{III}(bicapped\text{-}TPTCAM)]^{3-}$ [9]. Contrary to the preceding $M–O_6$ complexes, which have geometries intermediate between octahedral and trigonal prismatic, the present complexes have a strictly trigonal prismatic geometry.

The Fe(III)/Fe(II) reduction processes in the bicapped complexes occur at potentials (Table 19) slightly less negative than those of the monocapped analogues. Also in these cases, the electrode potentials vary with pH [54]. No electrochemical investigation (possibly in non-aqueous solvents) has been carried out in the positive region in search of the redox activity of the catechol ligands.

2.5.2. Ruthenium complexes

2.5.2.1. Tris(quinoidal) complexes. X-ray crystallography succeeded in resolving the two geometrical isomers of $[Ru\{1,2\text{-}O_2C_6H_2(3,5\text{-}Bu^t)_2\}_3]^0$, which arise from the asymmetry of the *tert*-butyl substituents [55,1e]. Fig. 16 illustrates the C_3 isomer (in which the substituents mutually occupy the same positions in the three ligands).

Ambiguity in the formulation of the ligands can arise from the fact that the C–O and C1–C2 bond lengths, in both the isomers, are intermediate between the semiquinonate and the catecholate nature of the ligands; this, in turn, causes ambiguity on the oxidation state of the metal. The statistical treatment [7] affords a Δ value of −1.35 for the *cis* isomer and −1.12 for the *trans* isomer, which could support the preferential assignment of semiquinonate to the ligands. In CH_2Cl_2 solution, it displays two reversible reduction processes ($E^{0'}_{0/-} = -0.52$ V; $E^{0'}_{-/2-} = -1.14$ V versus Fc/Fc^+) and two oxidation processes,

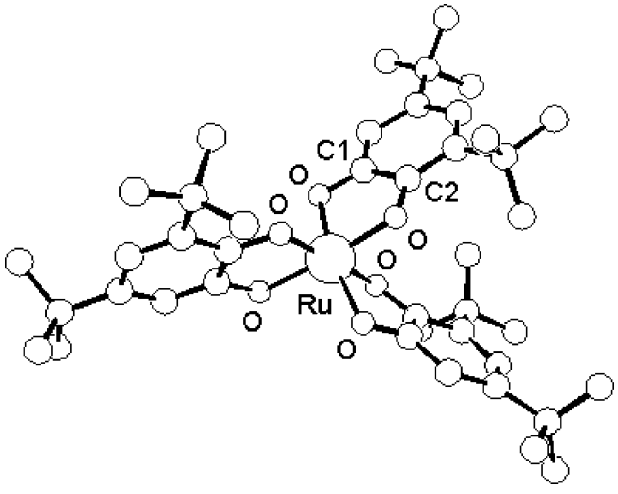

Fig. 16. X-ray crystal structure of C_3-$[Ru\{1,2\text{-}O_2C_6H_2(3,5\text{-}Bu^t)_2\}_3]^0$. Average bond lengths: Ru–O = 1.98 Å; C–O = 1.31 Å; C1–C2 = 1.43 Å (adapted from Ref. [55]).

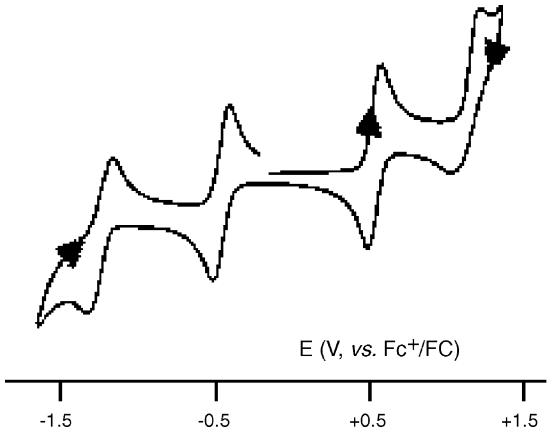

Fig. 17. Cyclic voltammogram recorded at a platinum electrode in CH_2Cl_2 solution of $[Os\{1,2\text{-}O_2C_6H_2(3,5\text{-}Bu^t)_2\}_3]^0$. Scan rate 0.1 V s^{-1} (adapted from Ref. [55]).

the first of which is chemically reversible ($E^{0'}_{0/+} = +0.35$ V), whereas the second is partially reversible ($E^{0'}_{+/2+} = +0.90$ V). Even though the first reduction and the two oxidation processes have been assigned. As ligand centred, and the second reduction as metal-centred [55], it cannot be excluded that all the processes are ligand centred.

2.5.3. Osmium complexes

2.5.3.1. Tris(quinoidal) complexes. The crystal structure of octahedrally distorted $[Os(1,2\text{-}O_2C_6H_4)_2]^0$ [56] and $[Os\{1,2\text{-}O_2C_6H_2(3,5\text{-}Bu^t)_2\}_3]^0$ [55,56] are known. As in the case of the ruthenium analogue, the C–O and C1–C2 distances in $[Os\{1,2\text{-}O_2C_6H_2(3,5\text{-}Bu^t)_2\}_3]^0$ are intermediate between the catecholate and semiquinonate nature of the ligands, thus causing ambiguity on the nature of the ligands and oxidation state of the metal. On the other hand, the statistical treatment too [7] is not firmly definitive ($\Delta = -1.42$).

As illustrated in Fig. 17, $[Os\{1,2\text{-}O_2C_6H_2(3,5\text{-}Bu^t)_2\}_3]^0$ undergoes in CH_2Cl_2 solution two reduction processes ($E^{0'}_{0/-} = -0.47$ V; $E^{0'}_{-/2-} = -1.24$ V versus Fc/Fc^+) and two oxidation processes ($E^{0'}_{0/+} = +0.52$ V; $E^{0'}_{+/2+} = +1.11$ V versus Fc/Fc^+), most of which display features of chemical reversibility. As in the case of the corresponding ruthenium complex, the first reduction and the two oxidation processes have been assigned as ligand-based, whereas the second reduction is thought to be metal-based [55].

2.6. Group 9 metalla-complexes (Co, Rh, Ir)

2.6.1. Cobalt complexes

2.6.1.1. Tris(quinoidal) complexes. As far as we know, the only mononuclear, homoleptic, quinoidal complex of cobalt which has been structurally characterised is the pseudooctahedral $[Co\{1,2\text{-}O_2C_6H_2(3,6\text{-}Bu^t)_2\}_3]^0$ [57]. As happens for $[Fe\{1,2\text{-}O_2C_6H_2(3,6\text{-}Bu^t)_2\}_3]^0$, the C–O and C1–C2 bond lengths indicate the semiquinonate character of the ligands (1.29 and 1.45 Å, respectively; Co–O = 1.88 Å; $\alpha = 56.5°$). The presence of the sterically encumbering *tert*-butyl groups in a position adjacent to

the oxygen atoms prevents the oligomerisation reactions which always affect the complexation reactions of semiquinone ligands (for instance, the dianion $[1,2\text{-}O_2C_6H_2(3,5\text{-}Bu^t)_2]^{2-}$ affords the tetramer $[Co(3,5\text{-}DBSQ)_2]_4$) [58]. No electrochemical data are available for $[Co(3,6\text{-}DBSQ)_3]$.

2.6.2. Rhodium complexes

2.6.2.1. Tris(quinoidal) complexes. Preliminary electrochemical data on $[Rh\{1,2\text{-}O_2C_6H_2(3,6\text{-}Bu^t)_2\}_3]^0$, which has been assigned as $[Rh^{III}(3,5\text{-}DBSQ)_3]$, show that it undergoes in 1,2-dichloroethane solution a series of ligand centred one-electron reduction processes, the first of which occurs at $E^{0'} = -0.23$ V versus SCE [59].

2.6.3. Iridium complexes

2.6.3.1. Tris(quinoidal) complexes. As in the case of $[Mn\{1,2\text{-}O_2C_6H_2(3,6\text{-}Bu^t)_2\}_3]$, which is assigned as $[Mn^{IV}(3,6\text{-}DBSQ)_2(3,6\text{-}DBCat)]$ (Section 2.4.1.2), the X-ray crystal structure of $[Ir\{1,2\text{-}O_2C_6H_2(3,6\text{-}Bu^t)_2\}_3]$ suggests a mixed-charge $[Ir^{V}(3,6\text{-}DBSQ)(3,6\text{-}DBCat)_2]$ formulation [1e]. No electrochemical data are available.

2.7. Group 10 metalla-complexes (Ni, Pd, Pt)

2.7.1. Nickel complexes

2.7.1.1. Bis(quinoidal) complexes. The square planar geometry of the neutral complex $[Ni^{II}\{1,2\text{-}O_2C_6H_2(3,6\text{-}Bu^t)_2\}_2]^0$ and its cyclic voltammetric profile are illustrated in Fig. 18 [60,61]. Based on the diagnostic structural parameters, the ligands possess a semiquinonate nature so that it is conceivable that the two separate one-electron additions ($E^{0'}_{0/-} = -0.38$ V, $E^{0'}_{-/2-} = -1.07$ V; versus Fc/Fc^+) are centred on the ligands, thus affording the corresponding catech olates.

One-electron chemical reduction seems to trigger the following internal redox change [61]:

$$[Ni^{II}(3,6-DBSQ)_2]^0 \overset{+e}{\rightleftarrows} [Ni^{II}(3,6-DBSQ)(3,6-DBCat)]^- \rightarrow [Ni^{III}(3,6-DBCat)_2]^-$$

$[Ni\{1,2\text{-}O_2C_6H_2(3,5\text{-}Bu^t)_2\}_2]^0$ is tetrameric in the solid state [62]. A square planar geometry is also exhibited by the dianions $[Ni(1,2\text{-}O_2C_6H_4)_2]^{2-}$ [63] and $[Ni(5\text{-}LICAM)]^{2-}$ [5-LICAM = *N*,*N*′-bis(2,3-dihydroxybenzoyl-1,7-diazaheptane)] [64]. A few significant structural parameters for the three complexes are compiled in Table 20. According to the usual diagnostic criteria, the dianions bear catecholate ligands. The $[Ni(Cat)_2]^{2-}$ undergoes a reversible one-electron oxidation

Table 20
Selected structural data (average bond lengths in Å) for a few bis-quinoidal nickel complexes

Complex	Ni–O	C–O	C1–C2	Reference
$[Ni\{1,2\text{-}O_2C_6H_2(3,6\text{-}Bu^t)_2\}_2]^0$	1.82	1.30	1.43	[60]
$[Ni(1,2\text{-}O_2C_6H_4)_2]^{2-}$	1.86	1.35	1.41	[63]
$[Ni(5\text{-}LICAM)]^{2-}$	1.87	1.33	1.43	[64]

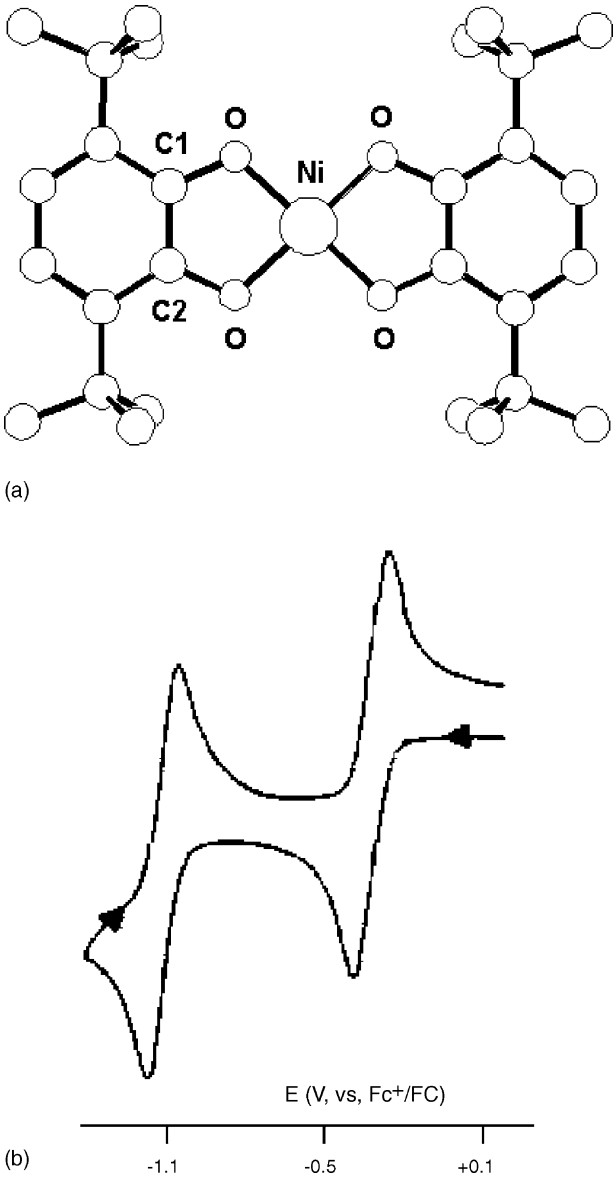

Fig. 18. X-ray crystal structure of $[Ni\{1,2\text{-}O_2C_6H_2(3,6\text{-}Bu^t)_2\}_2]^0$ (a) and its cyclic voltammetric profile in CH_2Cl_2 solution (b) (adapted from Refs. [60,61], respectively).

($E^{0'}_{2-/-} = -0.06$ V versus Ag/AgI) in dichloromethane solution. The same behaviour is exhibited by $[Ni(PhenCat)_2]^{2-}$ ($E^{0'}_{2-/-} = -0.38$ V) and $[Ni(Cl_4Cat)_2]^{2-}$ ($E^{0'}_{2-/-} = +0.48$ V) [42].

2.7.1.2. Comparison with the bis-dithiolene analogues. The X-ray crystal structures of both the dianion $[Ni(1,2\text{-}S_2C_6H_4)_2]^{2-}$ [65] and the monoanion $[Ni(1,2\text{-}S_2C_6H_4)_2]^{-}$ [66] are known. Table 21 compares the bond lengths of the redox couple $[Ni(1,2\text{-}S_2C_6H_4)_2]^{2-/-}$ with those of the catecholate dianion $[Ni(1,2\text{-}O_2C_6H_4)_2]^{2-}$.

In contrast to the easily detectable diagnostic structural features typical of the oxidation states of dioxolene ligands, dithiolene complexes in different oxidation states give rise to extended charge delocalisation which makes it difficult to state the metal-

Table 21
Structural comparison (average bond lengths in Å) between isostructural dioxolene (X = O) and dithiolene (X = S) nickel homologues

Complex	Ni–X	C–X	C1–C2	Counterion	Reference
$[Ni(1,2\text{-}O_2C_6H_4)_2]^{2-}$	1.86	1.35	1.41	$[Na]^+$	[61]
$[Ni(1,2\text{-}S_2C_6H_4)_2]^{2-}$	2.17	1.76	1.40	$[NMe_4]^+$	[65]
$[Ni(1,2\text{-}S_2C_6H_4)_2]^-$	2.15	1.74	1.40	$[NMPh]^{+a}$	[66a]
	2.15	1.74	1.40	$[FBzPy]^{+b}$	[66b]

[a] NMPh = *N*-methylphenazinium.
[b] *N*-4-Fluorobenzylpyridinium.

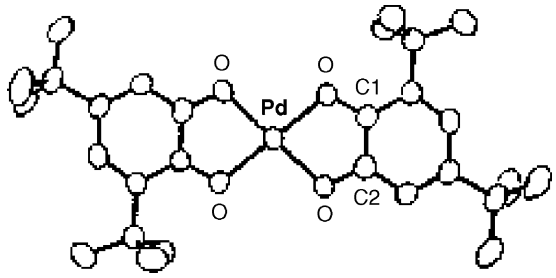

Fig. 19. X-ray crystal structure of $[Pd\{1,2\text{-}O_2C_6H_2(3,5\text{-}Bu^t)_2\}_2]^0$. Average bond lengths: Pd–O = 1.98 Å; C–O = 1.30 Å; C1–C2 = 1.43 Å (adapted from Ref. [67]).

centred (in the actual case, Ni(II)-to-Ni(III) conversion) or ligand-centred (in the actual case, benzene-1,2-dithiolate-to-benzene-1,2-dithione monoanion conversion) nature of the relative redox changes [2].

2.7.1.3. Tris(quinoidal) complexes. The only structurally characterised tris-quinoidal complex of nickel is $[Ni\{1,2\text{-}O_2C_6H_2(3,6\text{-}Bu^t)_2\}_3]^0$, which, based on the X-ray structural parameters, has been assigned as $[Ni(3,6\text{-DBQ})(3,6\text{-DBSQ})_2]$ [61]. No electrochemical data are available since, in solution, it releases free 3,6-DBQ transforming into $[Ni(3,6\text{-DBSQ})_2]$.

2.7.2. Palladium complexes

2.7.2.1. Bis(quinoidal) complexes. Fig. 19 shows the square planar geometry of $[Pd\{1,2\text{-}O_2C_6H_2(3,5\text{-}Bu^t)_2\}_2]^0$ [67]. The C–O and C1–C2 bond lengths are diagnostic of the semiquinonate form of the two ligands, which means that the complex can be described as $[Pd^{II}(3,5\text{-DBSQ})_2]$.

In CH_2Cl_2 solution, it displays two reversible reduction processes and one irreversible oxidation, which are assigned to the sequence:

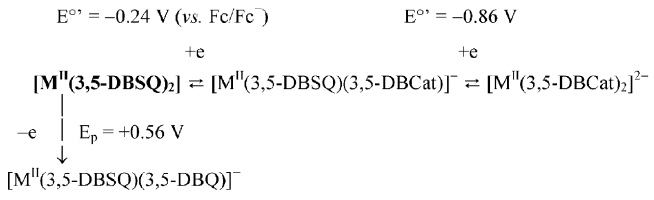

2.7.3. Platinum complexes

2.7.3.1. Bis(quinoidal) complexes. $[Pt\{1,2\text{-}O_2C_6H_2(3,5\text{-}Bu^t)_2\}_2]^0$ is isostructural with $[Pd\{1,2\text{-}O_2C_6H_2(3,5\text{-}Bu^t)_2\}_2]^0$ and is formulated as $[Pd^{II}(3,5\text{-DBSQ})_2]$ [67]. The similarity between the physico-chemical properties of $[Pd^{II}(3,5\text{-DBSQ})_2]$ and $[Pt^{II}(3,5\text{-DBSQ})_2]$ extends also to their redox behaviour. In fact, in CH_2Cl_2 solution, it undergoes the same sequence above illustrated for the palladium analogue (reduction processes: $E^{0'} = -0.06$ V, $E^{0'} = -0.80$ V; oxidation: $E_p = +0.69$ V (V versus Fc/Fc^+)) [67].

2.8. Group 11 metalla-complexes (Cu)

2.8.1. Copper complexes

2.8.1.1. Bis(quinoidal) complexes. While $[Cu\{1,2\text{-}O_2C_6H_2(3,5\text{-}Bu^t)_2\}_2]$ assumes a dimeric structure in the solid state [68], in solution it appears monomeric. In the solid state, each copper(II) ion has a distorted planar arrangement. The C–O and C1–C2 diagnostic distances (1.29 and 1.47 Å, respectively) indicate the semiquinonate nature of the ligands, or $[Cu(3,5\text{-DBSQ})_2]$ [68]. In CH_2Cl_2 solution, $[Cu(Cat)_2]^{2-}$ provides an irreversible one-electron oxidation [51]. Electrochemical investigation of MeCN solutions of $[Cu(3,5\text{-DBCat})_2]^{2-}$ and $[Cu(3,5\text{-DBCat})(3,5\text{-DBSQ})]^-$ have been reported [69].

2.9. Group 12 metalla-complexes (Zn)

2.9.1. Zinc complexes

2.9.1.1. Bis(quinoidal) complexes. Electrochemical information on $[Zn\{1,2\text{-}O_2C_6H_2(3,5\text{-}Bu^t)_2\}_2]^n$ ($n = +/0/-$) has been reported [70], but no structural data are available.

2.10. Metalla-complexes of lanthanides (Ce, Gd)

2.10.1. Cerium complexes

2.10.1.1. Tetrakis(quinoidal) complexes. The eight-coordinate dodecahedral geometry of $[Ce(1,2\text{-}O_2C_6H_4)_4]^{4-}$ is illustrated in Fig. 20 [10a]. The C–O and C1–C2 distances are diag-

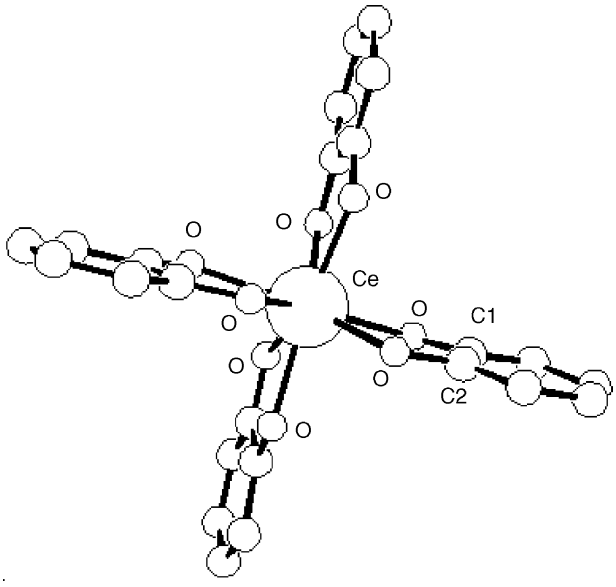

Fig. 20. X-ray crystal structure of $[Ce(1,2\text{-}O_2C_6H_4)_4]^{4-}$. Average bond lengths: Ce–O = 2.36 Å; C–O = 1.35 Å; C1–C2 = 1.40 Å (adapted from Ref. [10a]).

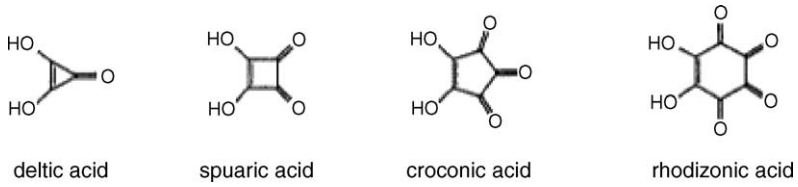

Scheme 6. Structure of oxo-carbon ligands.

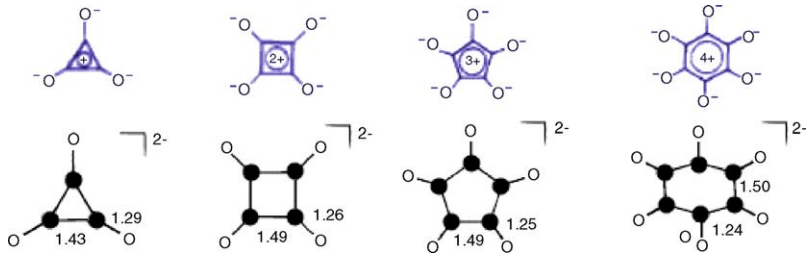

Scheme 7. Electronic delocalisation (and structural data) for the dianions of oxo-carbon ligands.

nostic of catecholate ligands, so that the tetranion is formulated as $[Ce^{IV}(Cat)_4]^{4-}$. In basic solution and in excess of catechol the tetraanion undergoes a chemically reversible one-electron reduction ($E^{0'} = -0.69$ V versus SCE), which is obviously assigned as $[Ce^{IV}(Cat)_4]^{4-}/[Ce^{III}(Cat)_4]^{5-}$ [10a]. The use of a mercury electrode likely prevented detection of ligand based oxidation processes. The required presence of free catechol to obtain a chemically reversible reduction means that the reduction is accompanied by release of free ligand.

2.10.2. Gadolinium complexes

2.10.2.1. Tetrakis(quinoidal) complexes. While the tris(quinoidal) complex of gadolinium(III) crystallizes as a dimer, which has been formulated as $[\{Gd(Cat)_3\}_2]^{6-}$, the tetraligand $[Gd(1,2\text{-}O_2C_6H_4)_4]^{5-}$, like $[Hf^{IV}(Cat)_4]^{4-}$ and $[Ce^{IV}(Cat)_4]^{4-}$, possesses an eight-coordinate dodecahedral geometry with catecholate type ligands [10b]. The pentaanion is hence formulated as $[Gd^{III}(Cat)_4]^{5-}$. No electrochemical data are available.

2.11. Metalla-complexes of actinides (Th, U)

2.11.1. Thorium complexes

2.11.1.1. Tetrakis(quinoidal) complexes. As with the previously discussed lanthanide complexes, $[Th(1,2\text{-}O_2C_6H_4)_4]^{4-}$ exhibits an eight-coordinate dodecahedral geometry with bond distances typical of catecholate complexes, and can be described as $[Th^{IV}(Cat)_4]^{4-}$ [71]. No electrochemical data are available.

2.11.2. Uranium complexes

2.11.2.1. Tetrakis(quinoidal) complexes. $[U(1,2\text{-}O_2C_6H_4)_4]^{4-}$ is isostructural with $[Th(1,2\text{-}O_2C_6H_4)_4]^{4-}$ and is formulated as $[U^{IV}(Cat)_4]^{4-}$ [71]. Also in this case, no electrochemical data are available.

3. Non-benzenoid ligands

There is a series of non-aromatic oxo-carbon ligands which may be potential candidates to mimic 1,2-quinoidal molecules (Scheme 6).

The π-electrons of their aromatic dianions are delocalised along the entire carbon cycle (aromaticity is supposed to decrease with increase of the ring size) [72], Scheme 7, so that they possess little tendency to behave as 1,2-bidentate ligands (commonly they act as bridging ligands between/among metal fragments).

In contrast, a potential candidate to mimic the coordination properties of 1,2-quinoidal ligands is the tropolonate monoanion [73], Scheme 8, the typical C–O and C1–C2 bond lengths of which approach the criteria for the semiquinonate ligand [74].

3.1. Tropolonate

3.1.1. Bis(tropolonate) complexes

The only X-ray structures of a metalla-bis(tropolonate) of which we are aware are those of the planar $[Cu(1,2\text{-}O_2C_7H_5)_2]^0$ (average bond lengths: Cu–O = 1.91 Å; C–O = 1.30 Å;

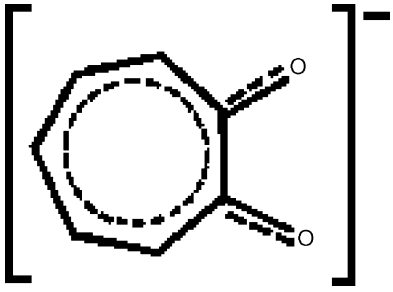

Scheme 8. Structure of the tropolonate monoanion.

Table 22
Selected structural data (bond lengths in Å, and twist angles in °) for $[M^{III}(trop)_3]$ complexes

Complex	M–O	C–O	C1–C2	α	Countercation	Reference
$[1,2\text{-}O_2C_7H_5]^-$	–	1.27	1.48	–	$[Na]^+$	[74b]
$[Sc(1,2\text{-}O_2C_7H_5)_3]^0$	2.10	1.30	1.46	33	–	[77a]
$[Mn(1,2\text{-}O_2C_7H_5)_3]^0$	2.00	1.29	1.45	≈49	–	[77b]
$[Fe(1,2\text{-}O_2C_7H_5)_3]^0$	2.01	1.29	1.46		–	[77c]

C1–C2 = 1.44 Å) [75], and the distorted octahedral $[MoO_2(1,2\text{-}O_2C_7H_5)_2]^0$ (average bond lengths: Mo–O_{trop} = 2.01 Å; C–O = 1.30 Å; C1–C2 = 1.45 Å) complexes [76]. No electrochemical data are available for the two species.

3.1.2. Tris(tropolonate) complexes

$[Sc(1,2\text{-}O_2C_7H_5)_3]^0$ possesses a pseudooctahedral geometry [77]. The pertinent structural parameters are collected in Table 22, together with those of the tris-tropolonates of other transition metals. As seen, the bond lengths maintain the typical features of the semiquinonate ligands. No electrochemical data are available on the redox properties of such derivatives.

3.1.3. Tetrakis(tropolonate) complexes

The X-ray structures of a series of tropolonate complexes of general formula $[M(1,2\text{-}O_2C_7H_5)_4]^n$ are known (M = Sc, $n = 1-$ [78a]; M = Zr, $n = 0$ [78b]; M = Hf, $n = 0$ [78c]; M = Nb, $n = 1+$ [78d]; M = Th, $n = 0$ [78e]). Their molecular structure is generally described in terms of approach to the dodecahedron or to the bicapped trigonal prism or to the square antiprism, which depends upon a set of diagnostic angles between the different faces of the central MO_8 polyhedron [79]. Table 23 summarizes a few structural data.

Given the coordination to the tropolonate monoanion, in all cases the diagnostic bond lengths approach those of semiquinonate ligands. In conclusion, based on the structural data available for the metal complexes of tropolonate and lacking any electrochemical studies, there is no support to assimilate tropolonates to dioxolenes as far as their redox propensity is concerned.

3.2. Deltate

The extensive π-electron delocalisation in cyclic oxo-carbon anions $C_nO_n^{n-}$ makes it unlikely that they can act as homoleptic chelating ligands. As a matter of fact, no metal complexes of deltate ligands have been prepared. The only structural information refers to deltic acid [80].

3.3. Squarate

The problem of electronic delocalisation also obviously holds for squarates [81]. The X-ray structures of squaric acid ($H_2C_4O_4$; 3,4-dihydroxycyclobut-3-ene-1,2-dione) [82], its acid monoanion ($[HC_4O_4]^-$) [83], and its dianion ($[C_4O_4]^{2-}$ [84]) are available, but no homoleptic transition metal complex has been structurally characterised. There are no literature reports on the electrochemical behaviour of the squarate dianion. This contrasts with the 1,2-dithiosquarate ligand ($[1,2\text{-}S_2C_4O_2]^{2-}$). The series $[M^{II}(1,2\text{-}S_2C_4O_2)_2]^{2-}$ (M = Ni, Cu, Pd, Pt) has been structurally characterised. From the electrochemical viewpoint, the data are rather scanty. The Pt complex exhibits a partially chemically reversible, one-electron oxidation [2].

3.3.1. Dicyanomethylene-squarate

Somewhat different is the situation of one substituted derivative of the squarate dianion (the class of substituted oxo-carbons is called pseudo oxo-carbons): the 3,4-bis(dicyanomethylene)cyclobutane-1,2-dione dianion ($cdcb^{2-}$), Scheme 9, the X-ray crystal structure of which is known [85].

It undergoes two separate, chemically reversible, one-electron oxidation processes ($E^{0'}$ = +0.68 and +1.47 V versus SCE, respectively) in MeCN solution [86], according to the sequence:

$$cdcb^{2-} \overset{-e}{\rightleftarrows} cdcb^{-} \overset{-e}{\rightleftarrows} cdcb$$

In spite of such redox activity and the expected aptitude to act as a chelating ligand in metal complexes, no mononuclear homoleptic transition metal complexes have so far been characterised.

Table 23
Selected structural data (bond lengths in Å) for $[M(trop)_4]^n$ complexes

Complex	M–O	C–O	C1–C2	Assigned geometry[a]	Counterion	Reference
$[Sc(1,2\text{-}O_2C_7H_5)_4]^-$	2.21	1.28	1.46	[b]	$[H]^+$	[78a]
$[Zr(1,2\text{-}O_2C_7H_5)_4]^0$	2.18	1.31	1.45	[c]	–	[78b]
$[Hf(1,2\text{-}O_2C_7H_5)_4]^0$	2.18	1.29	1.46	[c]	–	[78c]
$[Nb(1,2\text{-}O_2C_7H_5)_4]^+$	2.08	1.30	1.41	[b]	$[OH]^-$	[78d]
$[Th(1,2\text{-}O_2C_7H_5)_4]^0$	2.45	1.28	1.47	[d]	–	[78e]

[a] See text.
[b] Distorted bicapped trigonal prim.
[c] Nearly dodecahedron.
[d] Nine-coordinate.

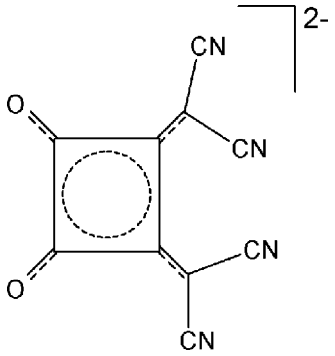

Scheme 9. Structure of the 3,4-bis(dicyanomethylene)cyclobutane-1,2-dione dianion.

3.4. Croconate

The X-ray structures of the croconate (4,5-dihydroxy-cyclopent-4-ene-1,2,3-trione) dianion ($[C_5O_5]^{2-}$) [84c,87], its acid monoanion ($[HC_5O_5]^-$) [87a,88] and the neutral croconic acid [89] are available. $[C_5O_5]^{2-}$ in non-aqueous solution shows two sequential one-electron oxidation processes with features of chemical reversibility on the cyclic voltammetric time scale [90]. The formal electrode potentials for the sequence $[C_5O_5]^{2-/-/0}$ are compiled in Table 24. Based on the separation of the two oxidation processes, $\Delta E^{0'}$, the monoanion $[C_5O_5]^-$ appears to be more stable in MeCN solution than in DMF solution.

3.4.1. Bis(croconate) complexes

A few X-ray structures of bis-croconate complexes have been reported, namely $K_{1.2}(H_3O^+)_{0.5}[Pt(C_5O_5)_2]$ [91a], $[NBu_4]_2[MoO_2(C_5O_5)_2]$ [91b], and $Na_2[M(C_5O_5)_2]$ (M = Cu, Ni; axial coordination of two water molecules) [91c], but no pertinent electrochemical data have been provided. As was the case of the dithiosquarate ligand, electrochemical data are available for a few metal complexes of the dithiocroconate ligand ($[1,2\text{-}S_2C_5O_3]^{2-}$), namely $[M^{II}(1,2\text{-}S_2C_5O_3)_2]^{2-}$ (M = Ni, Pd, Pt) and $[M^{III}(1,2\text{-}S_2C_5O_3)_3]^{3-}$ (M = Cr, Fe, Co). In general, such complexes undergo reversibly a one-electron oxidation and two one-electron reduction processes, which, based either on EPR spectroscopy or the nature of the central metal, are assigned as ligand-centred. It is evident that the two/three ligands are cooperatively dependent (otherwise, single two/three electron processes would have been found) [2].

3.4.2. Dicyanomethylene-croconates

Similarly to the squarate ligand, the carbonyl oxygen atoms of the croconate ligand can also be replaced by dicyanomethylene groups. A series of dicyanomethylene-croconates have been characterised, Scheme 10, which are brilliantly coloured derivatives regarded as cyanine dyes [92].

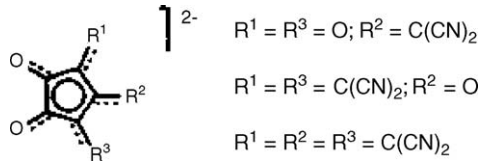

Scheme 10. Structures of a series of dicyanomethylene-croconates.

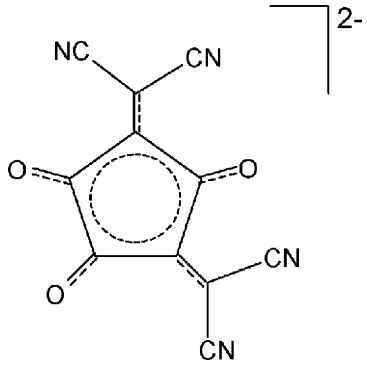

Scheme 11. Structure of croconate violet.

In particular, croconate violet {3,5-bis(dicyanomethylene) cyclopentane-1,2,4-trionate dianion, $[3,5\text{-}\{C(CN)_2\}_2\text{-}C_5O_3]^{2-}$}, Scheme 11, the crystal structure of which is known [93], appears pertinent to the present review paper.

Like $[C_5O_5]^{2-}$, croconate violet in non-aqueous solution displays two sequential one-electron oxidation processes with features of chemical reversibility on the cyclic voltammetric time scale [90a,b,d,e,94], but it also undergoes a one-electron reduction [90d,e,94]. The electrode potentials of such redox changes are compiled in Table 25.

3.4.2.1. Bis(croconate violet) complexes. Two bis(croconate violet) complexes have been structurally characterised: $K_2[Cu(3,5\text{-}\{C(CN)_2\}_2\text{-}C_5O_3)_2]$ [94] and $K_2[Co(3,5\text{-}\{C(CN)_2\}_2\text{-}C_5O_3)_2]$ [90d]. As illustrated in Fig. 21, which refers to $[Co(3,5\text{-}\{C(CN)_2\}_2\text{-}C_5O_3)_2]^{2-}$, in both cases the metal–croconate system is planar (with the two dicyanomethylene groups slightly rotated with respect to the plane (by about 5°)) while the coordination of the two water molecules provides an overall tetragonally distorted octahedral geometry to the central MO_6 core.

In both cases the croconate violet ligand coordinates in an unsymmetrical bidentate mode. A few selected interatomic distances for the two derivatives are reported in Table 26.

Table 24
Formal electrode potentials (V vs. SCE) for the one-electron oxidation processes of $[C_5O_5]^{2-}$ in non-aqueous solution

Complex	$E^{0'}_{2-/-}$	$E^{0'}_{-/0}$	$\Delta E^{0'}$	Solvent	Reference
$Li_2[C_5O_5]$	+0.23	+0.47	0.24	DMF	[90a,b]
$[PPh_4]_2[C_5O_5]$	+0.28	+0.81	0.53	MeCN	[90c]
	+0.11	+0.45	0.34	DMF	[90d]
$K_2[C_5O_5]$	+0.14	+0.55	0.41	DMF	[90e]

Table 25
Formal electrode potentials (V vs. SCE) for the electron transfers exhibited by $[3,5\text{-}\{C(CN)_2\}_2\text{-}C_5O_3]^{2-}$ in DMF solution

Complex	$E^{0'}_{2-/-}$	$E^{0'}_{-/0}$	$E^{0'}_{2-/3-}$	Reference
$Li_2[3,5\text{-}\{C(CN)_2\}_2\text{-}C_5O_3]$	+0.44	+0.86	–	[90a,b]
$K_2[3,5\text{-}\{C(CN)_2\}_2\text{-}C_5O_3]$	+0.45	+0.90	−1.49	[90d,e]

Table 26
Selected structural data (average bond lengths in Å) for the dianions $[M(3,5\text{-}\{C(CN)_2\}_2\text{-}C_5O_3)_2(H_2O)_2]^{2-}$

Complex	M–O1	M–O2	C–O(coordinated)	C1–C2	Reference
$[Co(3,5\text{-}\{C(CN)_2\}_2\text{-}C_5O_3)_2(H_2O)_2]^{2-}$	2.12	2.11	1.26	1.46	[90d]
$[Cu(3,5\text{-}\{C(CN)_2\}_2\text{-}C_5O_3)_2(H_2O)_2]^{2-}$	1.98	2.33	1.26	1.46	[94]

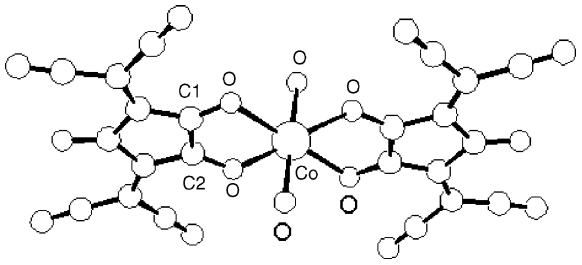

Fig. 21. X-ray crystal structure of $[Co(3,5\text{-}\{C(CN)_2\}_2\text{-}C_5O_3)_2(H_2O)_2]^{2-}$. $[K]^+$ counterion (adapted from Ref. [90d]).

As far as their redox activity is concerned, the cobalt complex shows two ligand centred reversible oxidation processes, Fig. 22, each one involving a two-electron step, which occur at potential values marginally different with respect to the free ligand [90d].

As a consequence of the complexation, the ligand centred reduction disappears (or is shifted at potential values more negative than the solvent discharge). No Co(II)-centred process is detected. As already discussed, the fact that the two croconate violet ligands oxidise at the same potential implies that no mutual electronic interaction exists [4]. Similar behaviour is observed for the copper complex, but for the fact that the ligand reduction must involve release and consequent reduction of Cu(II), in that a stripping peak (reoxidation of the copper metal deposed at the electrode surface) is recorded in the voltammetric backscan [94]. The electrode potential of the above discussed processes are reported in Table 27.

3.4.2.2. Tris(croconate violet) complexes. Fig. 23 illustrates the molecular structure of $[NBu_4]_4[Cu(3,5\text{-}\{C(CN)_2\}_2\text{-}C_5O_3)_3]$ [94].

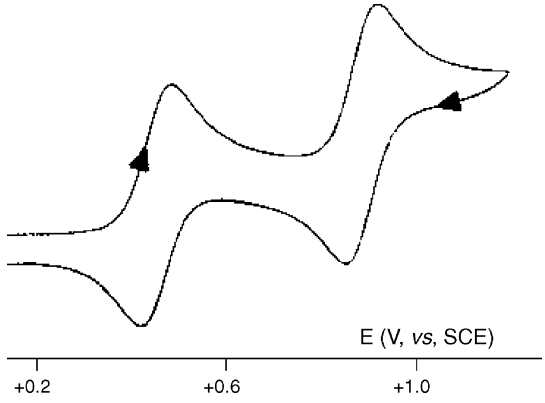

Fig. 22. Cyclic voltammogram recorded at a platinum electrode in DMF solution of $K_2[Co(3,5\text{-}\{C(CN)_2\}_2\text{-}C_5O_3)_2(H_2O)_2]$. Scan rate 0.1 V s^{-1} (adapted from Ref. [90d]).

Table 27
Formal electrode potentials (V vs. SCE) for the electron transfer processes exhibited by complexes $K_2[M(3,5\text{-}\{C(CN)_2\}_2\text{-}C_5O_3)_2]$ in DMF solution

M	$E^{0'}_{1st\ Ox}$	$E^{0'}_{2nd\ Ox}$	$E^{0'}_{Red}$	Reference
Co	+0.45	+0.93	–	[90d]
Cu	+0.48	+0.89	−1.47	[94]
$[3,5\text{-}\{C(CN)_2\}_2\text{-}C_5O_3]^{2-}$	+0.45	+0.90	−1.49	[90d,e]

Because of the probable Jahn–Teller effect, the octahedral geometry is notably distorted, so that each chelated ligand has its own bond lengths. The Cu–O distances span from 1.96 to 2.35 Å; the coordinated C–O groups range from 1.24 to 1.29 Å; the intradiol C1–C2 distances are 1.45 Å. As in the case of the corresponding bis(croconate violet) complex, the present complex also affords, in DMF solution, two ligand-centred, reversible oxidation processes ($E^{0'}$ = +0.47 and +0.90 V, respectively; V versus SCE) and a partially reversible reduction process ($E^{0'}$ = −1.50 V). Each process involves three-electrons and occurs at potential values essentially similar to those of the free ligand [94].

3.5. Rhodizonate

The crystal structure of the rhodizonate dianion $[C_6O_6]^{2-}$ is known [72g,95], but we are not aware of any electrochemical

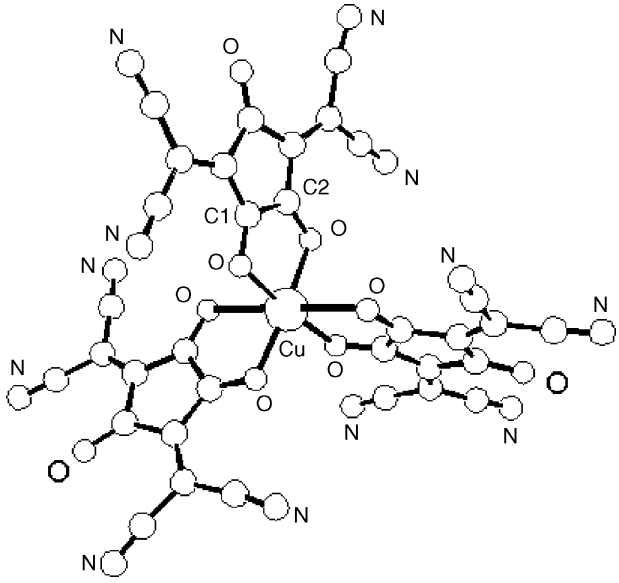

Fig. 23. X-ray crystal structure of $[NBu_4]_4[Cu(3,5\text{-}\{C(CN)_2\}_2\text{-}C_5O_3)_3]$ (adapted from Ref. [94]).

investigations on such a dianion or of the preparation of pertinent homoleptic metal complexes.

4. Conclusions

For many years, metal complexes of 1,2-dioxolene ligands has been an important topic in inorganic chemistry, mostly due to their extended electron-transfer ability, which makes them appealing from a theoretical point of view and of potential technological application [1]. Nevertheless, this rich redox aptitude has, in many cases, led to uncertainty in the derivation of the oxidation states of both metal and ligand. Much support can obviously be provided by joint electrochemical and structural studies, but conclusive evidence often also needs the contribution of further experimental techniques (e.g. magnetic investigation) as well as of theoretical studies.

We have also reviewed the electrochemical and structural aspects of metal complexes of tropolonate and oxo-carbon anion ligands, which are structurally and electronically reminiscent of the 1,2-dioxolenes. The chemistry of such "pseudo"-1,2-dioxolenes has long been neglected, but is recently recovering its rightful place.

Acknowledgements

P. Zanello acknowledges the financial support (PAR projects) and M. Corsini acknowledges a 5-year research grant from the University of Siena.

References

[1] (a) C.G. Pierpont, T.M. Buchanan, Coord. Chem. Rev. 38 (1981) 45–87;
(b) W.P. Griffith, Transition Met. Chem. 18 (1993) 250–256;
(c) C.G. Pierpont, C.W. Lange, Prog. Inorg. Chem. 41 (1994) 331–442;
(d) C.G. Pierpont, A.S. Attia, Collect. Czech. Chem. Commun. 66 (2001) 33–51;
(e) C.G. Pierpont, Coord. Chem. Rev. 219–221 (2001) 415–433;
(f) D.N. Hendrickson, C.G. Pierpont, Topics Curr. Chem. 234 (2004) 63–95.
[2] P. Zanello, E. Grigiotti, in: A.J.L. Pombeiro, C. Amatore (Eds.), Homoleptic, Mononuclear Transition Metal Complexes of 1,2-Dithiolenes: Updating their Electrochemical-to-Structural Properties, Fontis Media-Marcel Dekker Inc., 2004, pp. 3–70.
[3] (a) M.D. Ward, J.A. McCleverty, J. Chem. Soc., Dalton Trans. (2002) 275–288;
(b) S. Patra, B. Sarkar, S.M. Mobin, W. Kaim, G.K. Lahiri, Inorg. Chem. 42 (2003) 6469.
[4] P. Zanello, Inorganic Electrochemistry. Theory, Practice and Application, RSC, Cambridge, UK, 2003.
[5] (a) A. Levina, G.J. Foran, D.I. Pattison, P.A. Lay, Angew. Chem. Int. Ed. 43 (2004) 462;
(b) D.I. Pattison, A. Levina, M.J. Davies, P.A. Lay, Inorg. Chem. 40 (2001) 214.
[6] (a) V.H. Wunderlich, D. Mootz, Acta Cryst. B 27 (1971) 1684;
(b) A.L. Macdonald, J. Trotter, J. Chem. Soc., Perkin II (1973) 476;
(c) D.-N. Horng, J.-P. Chyn, K.-J. Shieh, J.-L. Chou, Y.-S. Wen, Acta Cryst. C 55 (1999) 652;
(d) G. Zanotti, A. Del Pra, Acta Cryst. B 34 (1978) 2997.
[7] O. Carugo, C. Bisi Castellani, K. Djinović, M. Rizzi, J. Chem. Soc., Dalton Trans. (1992) 837.
[8] B.A. Borgias, S.R. Cooper, Y.B. Koh, K.N. Raymond, Inorg. Chem. 23 (1984) 1009.
[9] T.B. Karpishin, T.D.P. Stack, K.N. Raymond, J. Am. Chem. Soc. 115 (1993) 182.
[10] (a) S.R. Sofen, S.R. Cooper, K.N. Raymond, Inorg. Chem. 18 (1979) 1611;
(b) G.E. Freeman, K.N. Raymond, Inorg. Chem. 24 (1985) 1410.
[11] S.R. Cooper, Y.B. Koh, K.N. Raymond, J. Am. Chem. Soc. 104 (1982) 5092.
[12] P.J. Bosserman, D.T. Sawyer, Inorg. Chem. 21 (1982) 1545.
[13] M.E. Cass, D.L. Greene, R.M. Buchanan, C.G. Pierpont, J. Am. Chem. Soc. 105 (1983) 2680.
[14] T.M. Dewey, J. Du Bois, K.N. Raymond, Inorg. Chem. 32 (1993) 1729.
[15] M.E. Cass, N.R. Gordon, C.G. Pierpont, Inorg. Chem. 25 (1986) 3962.
[16] (a) T.B. Karpishin, K.N. Raymond, Angew. Chem. Int. Ed. Engl. 31 (1992) 466;
(b) T.B. Karpishin, T.M. Dewey, K.N. Raymond, J. Am. Chem. Soc. 115 (1993) 1842;
(c) Z. Hou, T.D.P. Stack, C.J. Sunderland, K.N. Raymond, Inorg. Chim. Acta 263 (1997) 341;
(d) K.N. Raymond, Coord. Chem. Rev. 105 (1990) 135.
[17] A.R. Bulls, C.G. Peppin, F.E. Hahn, K.N. Raymond, J. Am. Chem. Soc. 112 (1990) 2627.
[18] M. Albrecht, S.J. Franklin, K.N. Raymond, Inorg. Chem. 33 (1994) 5785.
[19] K.N. Raymond, S.S. Isied, L.D. Brown, F.R. Fronzeck, J.H. Nibert, J. Am. Chem. Soc. 98 (1976) 1767.
[20] D.J. Gordon asnd, R.F. Fenske, Inorg. Chem. 21 (1982) 2907.
[21] S.R. Sofen, D.C. Ware, S.R. Cooper, K.N. Raymond, Inorg. Chem. 18 (1979) 234.
[22] C.G. Pierpont, private communication.
[23] (a) H.H. Downs, R.M. Buchanan, C.G. Pierpont, Inorg. Chem. 18 (1979) 1736;
(b) C.G. Pierpont, H.H. Downs, T.G. Rukavina, J. Am. Chem. Soc. 96 (1974) 5573.
[24] H.-C. Chang, T. Ishii, M. Kondo, S. Kitagawa, J. Chem. Soc., Dalton Trans. (1999) 2467.
[25] C.G. Pierpont, Inorg. Chem. 40 (2001) 5727.
[26] C.G. Pierpont, H.H. Downs, J. Am. Chem. Soc. 98 (1976) 4834.
[27] H.-C. Chang, H. Miyasaka, S. Kitagawa, Inorg. Chem. 40 (2001) 146.
[28] (a) N. Cheraïti, M.E. Brik, G. Kunesch, A. Gaudemer, J. Organomet. Chem. 575 (1999) 149 (and references therein);
(b) A.-K. Duhme, J. Chem. Soc., Dalton Trans. (1997) 773;
(c) A.-K. Duhme-Klair, D.C.L. de Alwis, F.A. Schultz, Inorg. Chim. Acta 351 (2003) 150 (and references therein);
(d) T. Palanché, S. Blanc, C. Hennard, M.A. Abdallah, A.-M. Albrecht-Gary, Inorg. Chem. 43 (2004) 1137 (and references therein).
[29] C.-M. Liu, E. Nordlander, D. Schmeh, R. Shoemaker, C.G. Pierpont, Inorg. Chem. 43 (2004) 2114.
[30] (a) V.V. Tkachev, L.O. Atovmyan, Coord. Chem. (USSR) (1976) 715;
(b) J.H. Reibenspies, K. Klausmeyer, D. Darensborg, Z. Kristallogr. 209 (1994) 761.
[31] W.P. Griffith, H.I.S. Nogueira, B.C. Parkin, R.N. Sheppard, A.J.P. White, D.J. Williams, J. Chem. Soc., Dalton Trans. (1995) 1775.
[32] (a) L.M. Charney, F.A. Schultz, Inorg. Chem. 19 (1980) 1527;
(b) L.M. Charney, H.O. Finklea, F.A. Schultz, Inorg. Chem. 21 (1982) 549.
[33] N. Yoshinaga, N. Ueyama, T. Okamura, A. Nakamura, Chem. Lett. (1990) 1655.
[34] C.G. Pierpont, R. Buchanan, J. Am. Chem. Soc. 97 (1975) 4912.
[35] S.M. Beshouri, I.P. Rothwell, Inorg. Chem. 25 (1986) 1962.
[36] T.S. Sheriff, P. Carr, B. Piggott, Inorg. Chim. Acta 348 (2003) 115.
[37] (a) J.A.R. Hartman, B.M. Foxman, S.R. Cooper, J. Chem. Soc., Chem. Commun. (1982) 583;
(b) D.H. Chin, D.T. Sawyer, W.P. Schaefer, C.J. Simmons, Inorg. Chem. 22 (1983) 752;
(c) J.R. Hartman, B.M. Foxman, S.R. Cooper, Inorg. Chem. 23 (1984) 1381.
[38] A.S. Attia, C.G. Pierpont, Inorg. Chem. 37 (1998) 3051.

[39] R. Ruiz, A. Caneschi, D. Gatteschi, C. Sangregorio, L. Sorace, M. Vázquez, Inorg. Chem. Commun. 3 (2000) 76.
[40] T.S. Sheriff, P. Carr, S.J. Coles, M.B. Hursthouse, J. Lesin, M.E. Light, Inorg. Chim. Acta 357 (2004) 2494.
[41] K.D. Magers, C.G. Smith, D.T. Sawyer, Inorg. Chem. 19 (1980) 492.
[42] S.E. Jones, D.-H. Chin, D.T. Sawyer, Inorg. Chem. 20 (1981) 4257.
[43] A. Davison, B.V. DePamphilis, A.G. Jones, K.J. Franklin, C.J.L. Lock, Inorg. Chim. Acta 128 (1987) 161.
[44] S.F. Colmanet, M.F. Mackay, Aust. J. Chem. 40 (1987) 1301.
[45] L.A. deLearie, R.C. Haltiwanger, C.G. Pierpont, J. Am. Chem. Soc. 111 (1989) 4324.
[46] (a) L.A. deLearie, C.G. Pierpont, J. Am. Chem. Soc. 108 (1986) 6393; (b) L.A. deLearie, R.C. Haltiwanger, C.G. Pierpont, Inorg. Chem. 26 (1987) 817.
[47] S.R. Boone, G.H. Purser, H.-R. Chang, M.D. Lowery, D.N. Hendrickson, C.G. Pierpont, J. Am. Chem. Soc. 111 (1989) 2292.
[48] A.S. Attia, B.J. Conklin, C.W. Lange, C.G. Pierpont, Inorg. Chem. 35 (1996) 1033.
[49] R.M. Buchanan, S.L. Kessel, H.H. Downs, C.G. Pierpont, D.N. Hendrickson, J. Am. Chem. Soc. 100 (1978) 7894.
[50] S.E. Jones, L.E. Leon, D.T. Sawyer, Inorg. Chem. 21 (1982) 3692.
[51] F. Röhrscheid, A.L. Balch, R.H. Holm, Inorg. Chem. 5 (1966) 1542.
[52] W.R. Harris, C.J. Carrano, S.R. Cooper, S.R. Sofen, A.E. Avdeef, J.V. McArdle, K.N. Raymond, J. Am. Chem. Soc. 101 (1979) 6097.
[53] (a) T.D.P. Stack, T.B. Karpishin, K.N. Raymond, J. Am. Chem. Soc. 114 (1992) 1512;
(b) S.J. Rodgers, C.-W. Lee, C.Y. Ng, K.N. Raymond, Inorg. Chem. 26 (1987) 1622.
[54] (a) T.J. McMurry, M.W. Hosseini, T.M. Garrett, F.E. Hahn, Z.E. Reyes, K.N. Raymond, J. Am. Chem. Soc. 109 (1987) 7196;
(b) T.M. Garrett, T.J. McMurry, M.W. Hosseini, Z.E. Reyes, F.E. Hahn, K.N. Raymond, J. Am. Chem. Soc. 113 (1991) 2965.
[55] S. Bhattacharya, S.R. Boone, G.A. Fox, C.G. Pierpont, J. Am. Chem. Soc. 112 (1990) 1088.
[56] M.B. Hursthouse, T. Fram, L. New, W.P. Griffith, A.J. Nielson, Transition Met. Chem. 3 (1978) 255.
[57] C.W. Lange, B.J. Conklin, C.G. Pierpont, Inorg. Chem. 33 (1994) 1276.
[58] R.M. Buchanan, B.J. Fitzgerald, C.G. Pierpont, Inorg. Chem. 18 (1979) 3439.
[59] E.S. Dodsworth, A.B.P. Lever, Chem. Phys. Lett. 172 (1990) 151.
[60] G.A. Abakumov, V.K. Cherkasov, M.P. Bubnov, O.G. Éllert, Yu.V. Rakitin, L.N. Zakharov, Yu.T. Struchkov, Yu.N. Saf'yanov, Bull. Acad. Sci. USSR Div. Chem. Sci. (Engl. Transl) 41 (1992) 1813.
[61] C.W. Lange, C.G. Pierpont, Inorg. Chim. Acta 263 (1997) 219.
[62] R.M. Buchanan, B.J. Fitzgerald, C.G. Pierpont, Inorg. Chem. 20 (1981) 1038.
[63] C. Brückner, D.L. Caulder, K.N. Raymond, Inorg. Chem. 37 (1998) 6759.
[64] S.-P. Huang, K.J. Franz, M.M. Olmstead, R.H. Fish, Inorg. Chem. 34 (1995) 2820.
[65] D. Sellmann, S. Fünfgelder, F. Knoch, M. Moll, Z. Naturforsch. B 46 (1991) 1601.
[66] (a) C. Mahadevan, M. Seshasayee, P. Kuppusamy, P.T. Manoharan, J. Cryst. Spectrosc. Res. 15 (1985) 305;
(b) J.-L. Xie, X.-M. Ren, C. He, Y. Song, C.-Y. Duan, S. Gao, Q.-J. Meng, Polyhedron 22 (2003) 299.
[67] G.A. Fox, C.G. Pierpont, Inorg. Chem. 31 (1992) 3718.
[68] (a) J.S. Thompson, J.C. Calabrese, J. Am. Chem. Soc. 108 (1986) 1903;
(b) O. Kahn, R. Prins, J. Reedijk, J.S. Thompson, Inorg. Chem. 26 (1987) 3557.
[69] S. Harmalker, S.E. Jones, D.T. Sawyer, Inorg. Chem. 22 (1983) 2790.
[70] M.E. Bodini, G. Copia, R. Robinson, D.T. Sawyer, Inorg. Chem. 22 (1983) 126.
[71] S.R. Sofen, K. Abu-Dari, D.P. Freyberg, K.N. Raymond, J. Am. Chem. Soc. 100 (1978) 7882.
[72] (a) F. Serratosa, Acc. Chem. Res. 16 (1983) 170–176;
(b) G. Seitz, P. Imming, Chem. Rev. 92 (1992) 1227–1260;
(c) G.A. Olah, J. Bausch, G. Rasul, H. George, G.K. Surya Prakash, J. Am. Chem. Soc. 115 (1993) 8060;
(d) P.V.R. Schleyer, K. Najafian, B. Kiran, H. Jiao, J. Org. Chem. 65 (2000) 426;
(e) D. Quiñonero, A. Frontera, P. Ballester, P.M. Deyà, Tetrahedron Lett. 41 (2000) 2001;
(f) G.M.A. Junqueira, W.R. Rocha, W.B. De Almeida, H.F. Dos Santos, Phys. Chem. Chem. Phys. 3 (2001) 3499;
(g) D. Braga, G. Cojazzi, L. Maini, F. Grepioni, New J. Chem. 25 (2001) 1221.
[73] F.A. Cotton, G. Wilkinson, Advanced Norganic Chemistry, John Wiley, 1988, p. 481.
[74] (a) Y. Sasada, I. Nitta, Acta Cryst. 9 (1956) 205;
(b) R. Shiono, Acta Cryst. 14 (1961) 42.
[75] (a) J.M. Robertson, J. Chem. Soc. 1222 (1951);
(b) W.M. Macintyre, J.M. Robertson, F.R.S. Zahrobsky, R.F. Zahrobsky, Proc. R. Soc. Sez. A 289 (1966) 161.
[76] W.P. Griffith, C.A. Pumphrey, A.C. Skapski, Polyhedron 6 (1987) 891.
[77] (a) T.J. Anderson, M.A. Neuman, G.A. Melson, Inorg. Chem. 13 (1974) 158;
(b) A. Avdeef, J.A. Costamagna, J.P. Fackler Jr., Inorg. Chem. 13 (1974) 1854;
(c) T.A. Hamor, D.J. Watkin, Chem. Commun. (1969) 440.
[78] (a) A.R. Davis, F.W.B. Einstein, Inorg. Chem. 13 (1974) 1880;
(b) A.R. Davis, F.W.B. Einstein, Acta Cryst. B 34 (1978) 2110;
(c) P.D. Tranqui, A. Tissier, J. Laugier, P. Boyer, Acta Cryst. B 33 (1977) 392;
(d) A.R. Davis, F.W.B. Einstein, Inorg. Chem. 14 (1975) 3030;
(e) V.W. Day, J.L. Hoard, J. Am. Chem. Soc. 92 (1970) 3626.
[79] (a) M.A. Porai-Koshits, M.A. Aslanov, Zh. Strukt. Khim. 13 (1972) 266;
(b) L.G. Guggenberger, E.L. Muetterties, J. Am. Chem. Soc. 96 (1977) 1748.
[80] D. Semmingsen, P. Groth, J. Am. Chem. Soc. 109 (1987) 7238.
[81] (a) J.-C. Trombe, J.-F. Petit, A. Gleìzes, Inorg. Chim. Acta 167 (1990) 69;
(b) C.-R. Lee, C.-C. Wang, Y. Wang, Acta Cryst. B 52 (1996) 966.
[82] (a) D. Semmingsen, Tetrahedron Lett. (1973) 807;
(b) Y. Wang, G. Stucky, J.M. Williams, J. C. S. Perkin II, (1974) 35;
(c) D. Semminsen, F.J. Hollander, T.F. Koetzle, J. Chem. Phys. 66 (1977) 4405.
[83] (a) D.P.C. Thackeray, R. Shirley, J. Cryst. Mol. Struct. 2 (1972) 159;
(b) R.J. Bull, M.F.C. Ladd, D.C. Povey, R. Shirley, Cryst. Struct. Commun. 2 (1973) 625;
(c) D. Semminsen, Acta Chem. Scand. A 30 (1976) 808.
[84] (a) W.M. Macintyre, M.S. Werkema, J. Chem. Phys. 42 (1964) 3563;
(b) V. Busetti, F. Marcuzzi, Z. Kristallogr. 212 (1997) 302;
(c) A. Ranganathan, G.U. Kulkarni, J. Phys. Chem. A 106 (2002) 7813.
[85] (a) H.E. Sprenger, W. Ziegenbein, Angew. Chem. Int. Ed. Engl. 6 (1967) 553;
(b) V. Busetti, B. Lunelli, J. Phys. Chem. 90 (1986) 2052;
(c) B. Lunelli, V. Busetti, J. Mol. Struct. 160 (1987) 287.
[86] G. Capobianco, G. Farnia, A. Gennaro, B. Lunelli, J. Electroanal. Chem. 142 (1982) 201.
[87] (a) N.C. Baenziger, J.J. Hegenbarth, D.G. Williams, J. Am. Chem. Soc. 85 (1963) 1539;
(b) N.C. Baenziger, J.J. Hegenbarth, J. Am. Chem. Soc. 86 (1964) 3250;
(c) Z. Sharshenalievna, F. Pishugin, G.L. Rosenthal, M.J. Strauss, Tetrahedron Lett. 31 (1990) 1797;
(d) J.D. Dunitz, P. Seiler, W. Czechtizky, Angew. Chem. Int. Ed. 40 (2001) 1779;
(e) C.-K. Lam, M.-F. Cheng, C.-L. Li, J.-P. Zhang, X.-M. Chen, W.-K. Li, T.C.W. Mak, Chem. Commun. (2004) 448.
[88] N.C. Baenziger, D.G. Williams, J. Am. Chem. Soc. 88 (1966) 689.
[89] D. Braga, L. Maini, F. Grepioni, Cryst. Eng. Commun. 6 (2001) 1.
[90] (a) L.M. Doane, A.J. Fatiadi, Angew. Chem. Int. Ed. 21 (1982) 635;
(b) L.M. Doane, A.J. Fatiadi, J. Electroanal. Chem. 135 (1982) 193;
(c) P.L. Fabre, P. Castan, D. Deguenon, N. Paillous, Can. J. Chem. 73 (1995) 1298;

(d) F. Dumestre, B. Soula, A.-M. Galibert, P.-L. Fabre, G. Bernardinelli, B. Donnadieu, P. Castan, J. Chem. Soc., Dalton Trans. (1998) 4131;
(e) P.-L. Fabre, F. Dumestre, B. Soula, A.-M. Galibert, Electrochim. Acta 45 (2000) 2697.
[91] (a) H. Toftlund, Chem. Scr. 17 (1981) 196;
(b) Q. Chen, S. Liu, J. Zubieta, Inorg. Chim. Acta 175 (1990) 241;
(c) C.-C. Wang, C.-H. Yang, G.-H. Lee, Inorg. Chem. 41 (2002) 1015.
[92] (a) A.J. Fatiadi, J. Am. Chem. Soc. 100 (1978) 2586;
(b) A.J. Fatiadi, J. Org. Chem. 45 (1980) 1338.
[93] V.L. Himes, A.D. Mighell, C.R. Hubbard, A.J. Fatiadi, J. Res. Nat. Bur. Stand (US) 85 (1980) 87.
[94] B. Soula, A.-M. Galibert, B. Donnadieu, P.-L. Fabre, Inorg. Chim. Acta 324 (2001) 90.
[95] M. Ito, R. West, J. Am. Chem. Soc. 85 (1963) 2580.